Project Number: JRB C007

Thermal Response Modeling of Fusible Link Activation in
Laboratory Simulated Wildfire Conditions

A Major Qualifying Project Proposal:

Submitted to the Faculty

Of the

Worcester Polytechnic Institute

In partial fulfillment of the requirement for the

Degree of Bachelor of Science

By

_____
Thomas J. DeMasi

_____
Michael P. Sheehan

Date: April 26, 2007

Approved:

_____
Professor Jonathan R. Barnett, Major Advisor

Abstract:

A thermal response model was developed for fusible link activation in wildfire conditions. Heat transfer parameters for this model were determined through experimental testing. Fusible links were tested in laboratory simulated wildfire conditions at the CSIRO Bushfire Research Laboratory in order to validate the developed model. This model was used to determine the potential use of fusible links for automatic actuation of wildfire doors and shutters.

Acknowledgements

Many have graciously assisted throughout the duration of this project. All help and contributions are greatly appreciated and extremely helpful. The following is a list of people that have aided in the completion of this project and understanding of the subject material:

1)   CSIRO CMMT – Financial Sponsor

2)   Professor Jonathan Ross Barnett – Academic Advisor

3)   Alex Webb – CSIRO Liaison and Advisor

4)   Nathan White – CSIRO Lab Assistance

5)   Lyndon MacIndoe - CSIRO Lab Assistance

6)   Paul Bowditch – CSIRO Lab Assistance

7)   Peter Haggard – CSIRO Lab Assistance

8)   Glenn Bradbury – CSIRO Lab Assistance

9)   David O'Brien – CSIRO Lab Assistance

10)   Vince Dowling – CSIRO Sponsor

11)   Chris Preston – CSIRO Lab Assistance

12)   Kahn Ho – CSIRO Lab Assistance

13)   CSIRO Workshop (Tony) - CSIRO

14)   Luke Connery – Tyco Fire and Security

15)   Jim Smalley – National Fire Protection Association liaison

Table of Contents

Table of Figures

Table of Tables

Nomenclature

List of Acronyms

AS	Australian Standard
CHP	Change of Phase Parameter
CMMT	CSIRO Manufacturing and Materials Technology
CRC	Cooperative Research Centers
CSIRO	Commonwealth of Scientific Industrial Research Organization
ICFME	International Crown Fire Modeling Experiment
FDI	Fire Danger Inidcator
FM	Factory Mutual
LPG	Liquefied Petroleum Gas
MIMS	Mineral-insulated metal sheath
MQP	Major Qualifying Project
NFPA	National Fire Protection Association
NIST	National Institute of Standards and Technology
RAL	Riley Air Link
RTI	Response Time Index
SFPE	Society of Fire Protection Engineers
UL	Underwriters Laboratory
WPI	Worcester Polytechnic Institute

List of Terms

Creep	Physical deformation
Link activation	Link separation
Flux	Incident radiation
Incident Radiation	Simulated radiation exposure
Profile	Data vs. time
Runge-Kutta Method	Numerical method for solving differential equations
R-Squared Analysis	Statistical indicator of a model's strength
View Factor	Radiation shape factor

Executive Summary

Australia's wildfires threaten many people's homes and businesses. Although many buildings and homes meet the prescribed construction levels of *Australian Standard 3959: Construction of Buildings in Bush Fire Areas*, there continues to be a need for additional research into alternative solutions which increase the protection from fire. The goal of this project was to develop a means of automatically closing an exterior fire door or shutter, which would prevent barrier failure of a window exposed to a wildfire.

Through the design process the most viable solution that was found was to use fusible links. A fusible link is comprised of two pieces of metal held together by a eutectic solder. This link is rated specified applied loadings and uses. These links would essentially hold open the fire door which would be pulled closed by a counterweight-pulley system when the fusible link activated. The intended use of the fusible links for this application goes beyond manufacturer activation guarantees because fusible links are designed for scenarios which do not include radiation exposures provided by wildfires. Experimental testing was necessary to test the fusible links to ensure that the fusible links would be applicable for this design specification.

Window performance objectives were determine based on results of existing literature released by the Bushfire Cooperative Research Centers (CRC) and documented performance levels of toughened glass exposed to radiation fluxes. This report noted specific failure times of windows that would be used in the construction of buildings in wildfire prone areas. These times translated to the experiments as critical activation times for the links for high and low intensity fires.

In order to predict link activation times a transient transfer heat model was created. This model was constructed using basic heat transfer concepts in combination with experimentally determined parameters for the incident radiation, change of phase (CHP) and conductance (C'). Experimental testing for the Incident Radiation, CHP, and C' parameters were reproductions of methods used by others. Incident Radiation was

experimentally determined using the experimental apparatus and obtaining the empirical data of the radiation profiles. Finding the CHP parameter determined the ratio of energy required by the heat of fusion to the total energy required to activate the link, similar work was done in 1981 by Evans and Madrzykowski. Determining the C' parameter reproduced the procedures used by Heskestad and Bill in their two-parameter thermal response work from 1987. Similar thermal response models had been done to simulate the thermal response of sprinklers in compartment fire scenarios; however no published work had been conducted to account for the activation of fusible links outside sprinkler applications.

This model was verified with experimental results measured at the CSIRO Fire Science and Technology site located in Highett, Victoria, Australia. Experimental testing was done on the fusible links using a radiant panel array and test rig which was capable of simulating actual wildfire conditions. Wildfire conditions and radiation exposures used in the experimental testing were derived from an evaluation of the International Crown Fire Modeling Experiment (ICFME). In experimental testing various radiation profiles were used in order to account for the range of possible radiation exposures present in wildfire hazards.In the experimental testing raditation exposures reaches as high as 40 kW/m^2, initial ambient air temperatures varied between 15°C and 35°C, and wind speeds which varied from test to test from 0 m/s to 10 m/s. Additionally, optimal and worst case link configurations (view factors) were tested along with best and worst case emissivities of the links. In this thermal response model the user is required to specify the radiation profiles, ambient air temperatures, cooling air speeds and specific link properties including, geometry and heat transfer properties including the response time index.

From the experimental testing and model results it was determined that the use of fusible links in fire door assemblies exposed to wildfire scenarios is largely dependent on the particular link. It was observed that for those tested, unaltered links activated after the time of barrier failure. However, when the links' were painted with black radiometer paint, ε= ~0.92, they activated well before window failure. Based on this finding it is

recommended that links potentially used in fire-door assembles exposed to wildfires be painted black with a paint of emissivity greater than ε= ~0.9.

From the model's results conclusions about the heat transfer process were made. It was found that in this application conduction loss from the thermal response element (solder) to the surrounding link plates and associated attachments was negligible. The dominant parameters influencing activation time were the emissivity of the link and the energy required by the solder's change of phase.

An accidental finding from this report was the potential use for plastic wire ties to act as the thermal response element. Plastic wire-ties were unintentionally tested and failed in all experiments prior to link activation. This suggests that wire-tires could potentially be a better means of activation. Thermal creep testing was done to determine the feasibility of their use in this application. In this test plastic wire-ties with an applied load of 10 kg were exposed to 50 ℃ temperatures over a period of three days, the deformation of the plastic ties was monitored. This experiment, while limited, indicates that thermal creep may not be a factor in the proposed application. It is recommended that additional testing be done to further verify the activation times of plastic wire-ties when exposed to wildfire conditions and to verify the minimal significance of thermal creep of plastic wire-ties in Australia environmental conditions.

1 Introduction – Objectives

The goal of this project was to find a method of automatically closing a fire door or shutter assembly that prevents barrier failure of windows when exposed to wildfire conditions. The design process indicated that fusible links were the most viable solution. The performance objective was to ensure that fusible links would activate closing a fire door or shutter prior to barrier failure of windows.

The performance of fusible links in wildfire conditions was determined experimentally using test apparatus located at the CSIRO Fire and Technology Research Laboratory. The test apparatus was capable of simulating wildfire conditions. Experimental data was then used to calibrate a computer model accounting for energy storage, incident radiation, convective cooling, conductive losses, heat of fusion energy, and radiation losses of the fusible link. This model was then used to accurately predict the activation times of fusible links when exposed to various and extreme conditions. These results verified the use of fusible links in fire door and shutter applications when exposed to wildfire hazards. In circumstances where links failed to activate, alterations were made to the emissivity of the links to ensure activation.

2 Literature Review

2.1 *Radiation Exposures*

There is limited data available in the literature that documents wildfire radiation exposures. The predominant work was a result of the International Crown Fire Modeling Experiment (ICFME). The ICFME experiment was conducted with the objective of obtaining measurements of radiant intensity, air temperature and convective energy transfer in large scale experimental crown fires. In the experiment a site located in Canada consisting of 68-year-old jack pine stands (*Pinus banksiana*) averaging 13 m in height with an under-story of black spruce (*Picea mariana*). Experimental sites were surrounded by shrub dominated meadows varying from 0.5 to 1 km in width (Butler, 2004). Each experimental site was between 75 m x 75 m and 150 m x 150 m in area (Butler, 2004). These sites were ignited, resulting in actual wildfire conditions where air temperatures and radiant intensities were recorded at various heights.

In 2006, the Bushfire CRC released a report documenting the performance of windows when exposed to radiant intensities of wildfires. In the CRC report various window types were exposed to experimentally simulated wildfire conditions. In this report a number of different radiation profiles were used. The report primarily used two profiles, a slow profile and a fast profile. The fast profile effectively simulated the actual wildfire conditions measured in the ICFME, as depicted in Figure 2-1. The slow profile simulated the worst case scenario in terms of window performance (CRC, 2004) depicted in Figure 2-2.
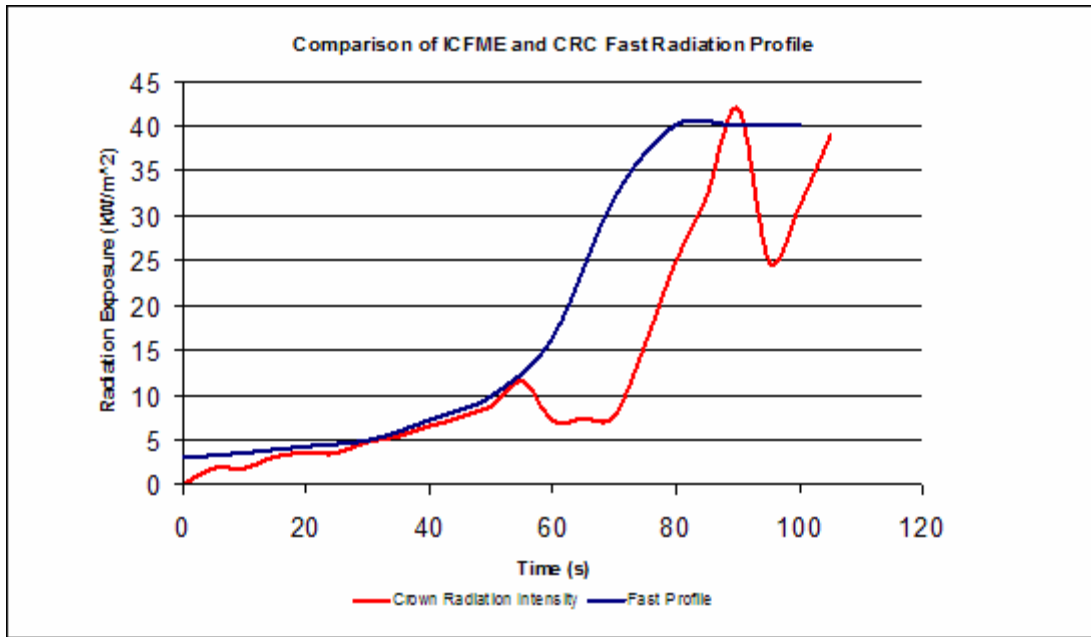
Figure 2-1: CRC Fast Profile vs. ICFME Experimental Results

In the ICFME it was found that the radiant intensities would exceed 40 kW/m^2 (Butler, 2004). The performance specification the window and the link, discussed in Section 2.2, required that the link activate prior to the time that the radiant intensities of the ICFME exceeded 40 kW/m^2. The CRC slow profile was selected for evaluation because it accounted for the worst possible scenario in terms of window performance, discussed in Section 2.2.
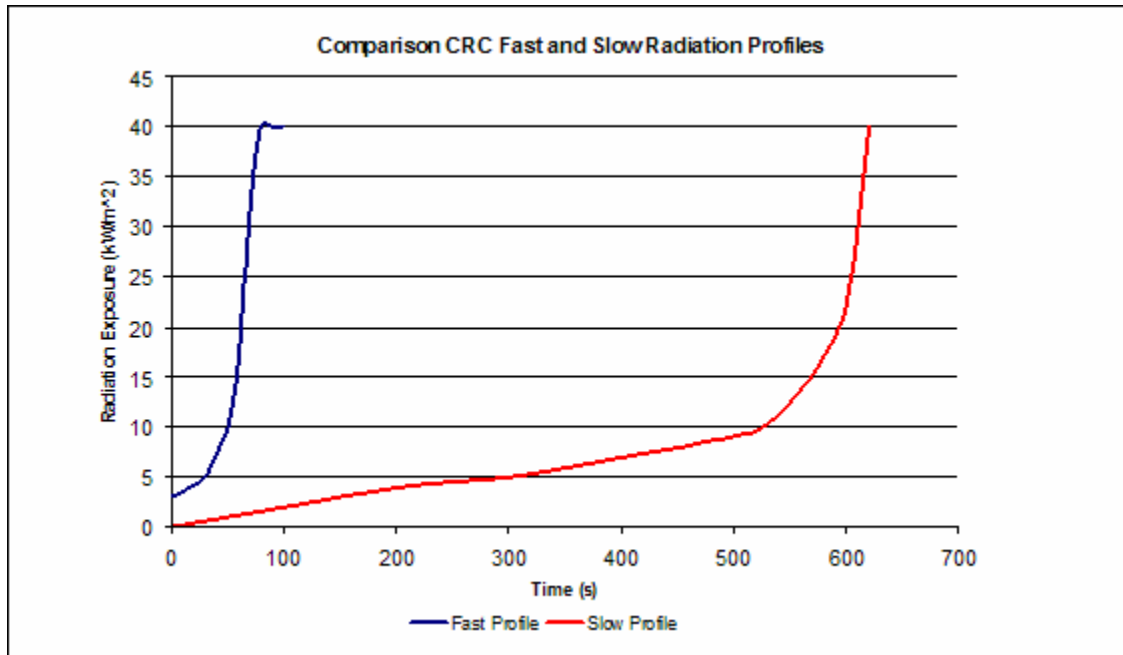
Figure 2-2: Selected Radiation Profiles

2.2 Window Performance Specification

The Bushfire CRC report found that 5 mm toughened glass windows maintained barrier integrity for the longest periods of exposure when mounted in an aluminum frame (CRC, 2004). In cases where windows were mounted in wooden frames there were a number of failures caused by ignition of the wooden frame (CRC, 2004). From this finding it is suggested that aluminum framed windows be used.

2.2.1 Slow Profile

In the Bushfire CRC's experimental testing fourteen tests on five millimeter toughened glass windows mounted in aluminum frames were exposed to the slow radiation profile, discussed in Section 2.1 (CRC, 2004). In the testing a window failure was considered to be when the window cracked, shattered or flaming of the window frame or associated seals occurred. In the testing of the five millimeter toughened glass windows the first failures occurred at six hundred eighty seconds. The mode of failure was window seal catching fire. Similar modes of failure occurred to other test specimens (CRC, 2004). In cases where windows did not fail they were put through the radiant exposure testing again. In one case a window specimen was tested three times and failed by means of shattering at five hundred eighty seconds into the third test.

4

As a result of the findings of the CRC report on window performance the required activation times of fusible links could be specified. Assuming a five millimeter toughened glass window mounted in an aluminum frame is used it is required that the fusible links must activate before five hundred and seventy seconds when exposed to the slow radiation profile. This specification requires that links activate before window failure, thereby closing a fire door or shutter and protecting the window from failure.

2.2.2 Fast Profile

The Bushfire CRC report also tested ten five-millimeter toughened glass windows mounted in aluminum frames using the fast profile, discussed in Section 2.1. In these tests none of the windows failed during the test, however failure did occur upon the cooling of the windows (CRC, 2004).

As a result of the findings of the CRC report the performance specifications of fusible links could be specified in part. One limitation of the CRC testing was the intensity of the radiation exposures, in the testing the windows were only tested up to 40 kW/m^2 in most cases. Evaluating the findings of the ICFME report, shown in Figure 2-1 it is clear that wildfire radiation exposures exceed 40 kW/m^2. Evaluating Figure 2-1 shows that incident radiation exposures reach 40 kW/m^2 at approximately 85 seconds. Considering the limitations of the Bushfire CRC report this time serves as the upper limit of the performance based design specification. As a result, assuming a 5 mm toughened glass window mounted in an aluminum frame is used in the application, it is required that the fusible links activate before 85 seconds.

2.3 Thermal Response Models of Others

There has been much work done to create thermal response models describing automatic sprinkler response. The original model was known as the one parameter model, and introduced the characteristic response time index, RTI (Heskestad and Smith, 1976). In this model it is assumed that the heat sensitive element is heated purely by convection and that all of the heat transferred to the element is stored within the thermal element.

The model also assumed that the heating of the thermal element is done isothermally; therefore the temperature distribution within the element is uniform. The one-parameter model was later improved upon resulting in the two-parameter model which added a term accounting for conductive losses from the thermal element to the sprinkler fitting (Heskestad and Bill, 1987). This model was an improvement but did not account for the additional energy that is required to overcome the heat of fusion for solder type sprinklers. A three-parameter model was later created using the fundamentals of the one and two-parameter models. The third parameter accounted for the energy required for the heat of fusion or change of phase parameter (Gustafsson, 1988).

In order to create thermal response models of particular sprinklers experimental testing was required in order to account for the unknown parameters; the response time index (RTI), the conductance (C') and the change of phase parameter (CHP). This testing consisted of multiple plunge tests or a combination of plunge tests and ramp tests.

2.3.1 One Parameter Model

The one-parameter model was developed by Heskestad and Smith in 1976. Equation (1) was the basic equation used to create this model. The model assumed a lumped heat capacity (uniform temperature distribution within the link) and accounts for convective heating (Heskestad and Smith, 1976).

$$mc\frac{dT_E}{dt} = hA(T_G - T_E)$$

$$
\begin{aligned}
&m = \text{Mass (kg)}\\
&c = \text{Specific Heat } (\frac{\text{J}}{\text{kg.}^oC})\\
&h = \text{Convective Heat Transfer Coefficient } (\frac{\text{W}}{\text{m}^2.^oC})\\
&A = \text{Area (m}^2)\\
&T_E = \text{Temperature of the Element } (^oC)\\
&T_G = \text{Temperature of Gas } (^oC)
\end{aligned}
$$

(1)

In creating this model, Heskestad and Smith defined the time constant τ, which is defined in (2) (SFPE, 2003).

$$\tau = \frac{hA}{mc}$$

h = Convective Heat Transfer Coefficient ($W/m^2 \cdot {}^oC$)

A = Area

m = Mass (kg)

c = Specific Heat ($J/kg \cdot {}^oC$)

(2)

The convective heat transfer coefficient h, present in τ is a function of the velocity of the gases flowing past the thermal element (Incorpera, 2005). Heskestad and Smith determined that h, and consequently τ are proportional to the square root of the velocity of the gases passing the thermal element (SFPE, 2003). As a result, this relationship was expressed as the characteristic response time index (RTI), as shown in (3).

$$RTI = \tau \cdot \mu^{1/2}$$

μ = Gas Velocity (m/s)

$$\tau = \frac{m \cdot c_p}{h \cdot A}$$

m = mass (kg)

c_p = Specific Heat ($J/kg \cdot {}^oC$)

h = Convection Coefficient

A = Area

(3)

Equation (2) and Equation (3) can be substituted into Equation (1) to derive an equation representing the temperature over time, as shown in Equation (4). In order to solve this equation it is required to experimentally determine the value of RTI using either the results from a plunge test or a ramp test.

$$\frac{d(\Delta T_E)}{dt} = \frac{\sqrt{\mu}}{RTI} \left(\Delta T_G - \Delta T_E \right)$$

μ = Gas Velocity ($\sfrac{m}{s}$)

RTI = Response Time Index

$\Delta T_G = T_G - T_\infty \ (^oC)$

$\Delta T_E = T_E - T_o \ (^oC)$

(4)

2.3.2 Two-Parameter Model

Background and Derivations

In 1987, Heskestad and Bill improved the one-parameter model creating the two-parameter which took into account the conductive losses from the thermal response element to the sprinkler fitting (Heskestad and Bill, 1987). This model again assumed a uniform temperature distribution within the link. The basic heat balance equation for the two parameter model is given by Equation (5).

$$mc\frac{dT_E}{dt} = hA(T_G - T_E) - C'(T_E - T_o)$$

m = Mass (kg)

c = Specific Heat ($\sfrac{J}{kg \cdot {}^oC}$)

T_E = Element Temperature (^oC)

h = Convection Coefficient ($\sfrac{W}{m^2 \cdot {}^oC}$)

T_G = Temperature of gas in plunge test (^oC)

C' = Conductance ($\sfrac{W}{{}^oC}$)

(5)

As done with the one parameter model, Equation (2) and Equation (3) are inserted into the heat balance equation to obtain an equation representing the temperature, relative to ambient conditions, of the link of the time, given by Equation (6) (Ingason, 1993).

$$\frac{d(\Delta T_E)}{dt} = \frac{\sqrt{\mu}}{RTI}\left[\Delta T_G - (1 + \frac{C}{\sqrt{\mu}})\Delta T_E\right]$$

ΔT_E = Element Temperature with respect to Ambient Temperature ($^O C$)

μ = Gas Velocity in Plunge Test (m/s)

RTI = Response Time Index ($m^{1/2} s^{1/2}$)

$\Delta T_G = T_G - T\infty$ ($^O C$)

$\Delta T_E - T_o$ ($^O C$)

C = Unknown Conductivity Term $m^{1/2} s^{1/2}$

(6)

In this equation there are two unknowns; RTI and conductance (C'). In order to solve for the temperature, it is required to experimentally determine the values of RTI and C'. This is done by creating a system of equations using the experimental results from a ramp test and a plunge test.

System of Equations

Plunge Test Equation (Equation 1)

The analytical solution to Equation (6) is shown in Equation (7), this equation can be rearranged as shown in Equation (8). This represents the equation required to solve for the unknown value of the Response Time Index (RTI) which makes up one of the two unknowns in the system of equations required to solve for conductivity (C), which is then used to solve for the Conductance parameter (C') using (14). The experimental results of a plunge test are used as inputs equation (8).

$$\Delta T_E = \frac{\Delta T_E}{(1+\frac{C}{\sqrt{\mu}})}\left[1 - e^{\frac{-(1+\frac{C}{\sqrt{\mu}})\sqrt{\mu}t}{RTI}}\right]$$

(7)

$$RTI = \dfrac{-(1+\dfrac{C}{\sqrt{\mu}})\sqrt{\mu}\cdot t_{op}}{\ln\left[1-\dfrac{(1+\dfrac{C}{\sqrt{\mu}})\cdot \Delta T_{E-op}}{\Delta T_G}\right]}$$

(8)

$$\Delta T_G = T_G - T_\infty \,(^oC)$$
μ=Velocity of gas in plunge apparatus $(^m/_s)$
t_{op}=Time of link activation in plunge test (seconds)
$\Delta T_{E\text{-}op}$=$T_{Specified\ Activation\ Temperature}-T_o$
C=Unknown Conductivity Term
RTI = Unknown Response Time Index

Ramp Test Equation (Equation 2)

In order to derive an equation based on the experimental results provided by a ramp test
Equation (6) must be modified to account for the changing temperature in the ramp test.
The process of accounting for the varying temperature requires a substitution, shown in
Equation (9) (Heskestad and Bill, 1987). Applying this substitution in Equation (6)
results in Equation (10).

$$\Delta T_G = \beta t$$

(9)

β = Rate of Temperature Rise $(^oC/_s)$
t = time (seconds)

$$\frac{d(T_E)}{dt} = \frac{\sqrt{\mu}}{RTI}\left[\beta t - (1+\frac{C}{\sqrt{\mu}})\cdot \Delta T_E\right]$$

(10)

The analytical solution to Equation (10) is represented by Equation (11) (Inguson, 1993).
This equation can be further simplified by the assumption that if the response time of a
sprinkler is long enough when compared to the value of the response time index, the

exponential term in Equation (11) can be neglected resulting in Equation (12) (Gustafsson, 1988).

$$\Delta T_E = \frac{\beta}{(1+\frac{C}{\sqrt{\mu}})}\left[t - \frac{RTI}{(1+\frac{C}{\sqrt{\mu}})\sqrt{\mu}}\left(1 - e^{\frac{-(1+\frac{C}{\sqrt{\mu}})\sqrt{\mu}t}{RTI}} \right) \right] \tag{11}$$

$$\Delta T_E = \frac{\beta}{(1+\frac{C}{\sqrt{\mu}})}\left[t - \frac{RTI}{(1+\frac{C}{\sqrt{\mu}})\sqrt{\mu}} \right] \tag{12}$$

Equation (12) represents the second of the two equations required to solve for the unknown values of RTI and C. The results of a ramp test are used as inputs in this equation.

$$RTI = (1+\frac{C}{\sqrt{\mu}})\sqrt{\mu}\left[\frac{(1+\frac{C}{\sqrt{\mu}})\cdot \Delta T_{E-op}}{\beta} - t_{op} \right]$$

$$\Delta T_{E\text{-}op} = T_{\text{Specified Activation Temperature}} - T_o \, (^oC)$$

$$t_{op} = \text{Time of link activation in ramp test (seconds)} \tag{13}$$

$$\beta = \text{Rate of Temperature Rise in Ramp Test} \, (^oC\!/\!s)$$

$$\mu = \text{Gas velocity in ramp test apparatus} \, (m\!/\!s)$$

$$C = \text{Unknown Conductivity Term}$$

$$RTI = \text{Unknown Response Time Index}$$

System of Equations Results

After solving the values of RTI and conductivity (C), the conductance term (C') can be determined using Equation (14). The value of the conductance (C') can then be plugged into the thermal response model shown in Equation (5).

$$C' = C\frac{mc}{RTI}$$

C = Unknown Conductance Term
C' = Conductance ($W/{}^oC$)
RTI = Respnse Time Index
m = Mass of Element (kg)
c = Specific Heat of Element ($J/{kg \cdot {}^oC}$)

(14)

2.3.3 Three-Parameter Model

The two-parameter model defined by Heskestad and Bill did not account for the energy required for the solder of a sprinkler to undergo a eutectic phase change (Ingason, 1993). In 1988, the change of phase parameter (CHP) was accounted for by Gustafsson in the three-parameter model. In this model the two parameter model represented by Equation (5), defined by Heskestad and Bill is valid until the thermal element reaches the time of phase transition (Gustafsson, 1988). At the time of phase transition, Equation (15) becomes the governing equation in the model until the time of sprinkler activation (Gustafsson, 1988).

The change of phase parameter used by Gustafsson is equal to the parameter previously defined by Evans and Madrzykowski (Ingason, 1993). In the work of Evans and Madrzykowski, it was found that the temperature of the link's thermal element is constant from the onset of phase transition to link rupture (Evans and Madrzykowski, 1981). Evans and Madrzykowski derived that the convective energy to the link during this time interval represented by (15) (Evans and Madrzykowski, 1981).

$$\Delta E = hA(\Delta T_G - \Delta T_{E-op}) \cdot (t_r - t_p)$$

ΔE = Phase change energy transfer

h = Convective Heat Transfer Coefficient ($W/m^{2 \cdot o}C$)

A = Area (m^2)

$\Delta T_G = T_G - T_\infty$

$\Delta T_{E-op} = T_{\text{Specified Activation Temperature}} - T_o$

t_r = Time to link rupture

t_p = Time until phase change

(15)

Evans and Madrzykowski conducted experiments to determine the fraction of energy involved with link fusion. In order to determine this value a fusible link automatic sprinkler was placed in an oven at a temperature higher than the activation temperature of the sprinkler. The temperature of the oven and the temperature of the solder were recorded over time. The results indicated that the temperature of the solder would increase until the activation temperature. At this point the temperature of the solder would remain constant until link activation (Evans and Madrzykowski, 1981). The reason the temperature of the solder remains constant is because it undergoes a phase change. The results from the test were plotted, as depicted in Figure 2-3.
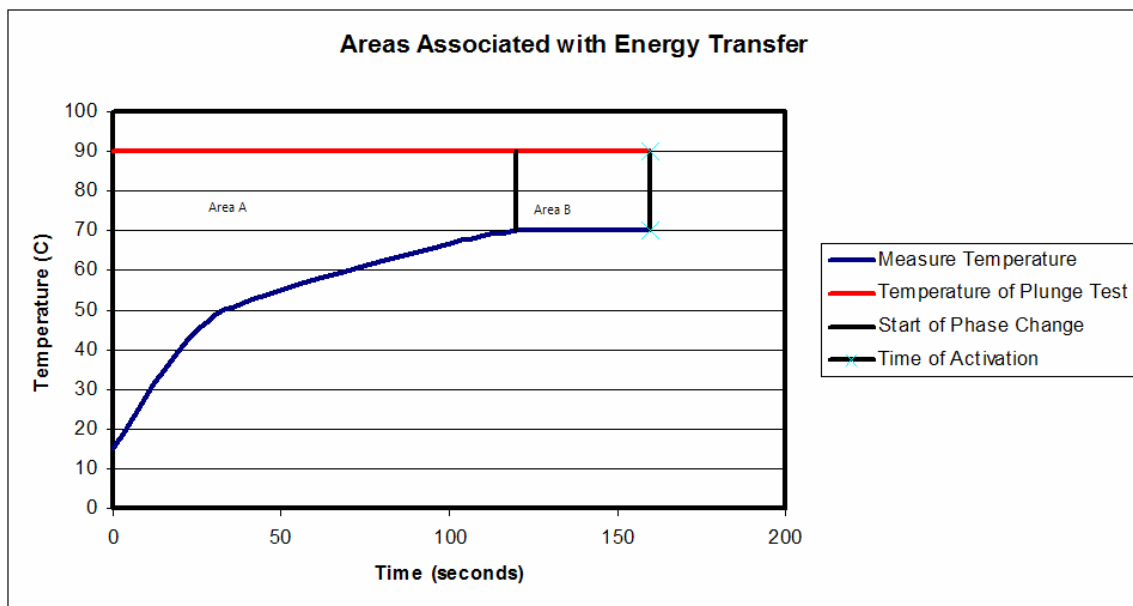
Figure 2-3: Sample Graphical Results for Fusion to Rupture Energy Ratio

From the experimental results Evans and Madrzykowski were able to determine the fraction of the total energy transferred to the link required to rupture the link. This was done using plotted results and by finding the areas between the oven temperature and the measured temperature of the solder. The first area (Area A) is the area between the curves originating at the time of sprinkler insertion into the oven until the initiation of the phase change. The second area (Area B) is the area between the curves originating at the time of phase change until the time of link activation. Equation (16) was used to determine the fraction of total energy required to account for the heat of fusion of the sprinkler (Evans and Madrzykowski, 1981).

$$\text{Fraction of Energy involved in link fusion} = \frac{\text{Fusion Energy}}{\text{Rupture Energy}} = \frac{\text{Area A}}{\text{Area A} + \text{Area B}}$$

(16)

Area A = Area between the curves until the link reaches the specified activation temperature
Area B = Area between the curves after reaching the specified activation temperature and the actual activation time

In their results Evans and Madrzykowski concluded that the energy associated with the fusion of a link could be as much as 31% of the total energy transfer needed to rupture the link (Evans and Madrzykowski, 1981).

2.4 Existing Link Descriptions

2.4.1 Riley Air Link (70°C Activation)

The Riley Air Link is a two part fusible link, made of two symmetrical rectangular brass plates held together by a eutectic solder. The link is fused together with solder that undergoes a phase change at 70°C. Where the link is fused each brass plate has a rectangular hole cut in it, these holes overlap when fused together. A brass cylinder is suspended in the rectangular hole with solder. Solder is also applied in between the two plates and the brass cylinder. The surface of the exposed brass is a brown burnished color. This link is rated for a maximum load of 40kg and a minimum load of 10kg. This link manufactured in Melbourne, Australia and is not Underwriters Laboratories (UL) listed or a Factory Mutual (FM) approved link. Specific link data can be seen in Table

2-1 and a photo of Riley Air Link activated (left) and un-activated (right) can be seen in Figure 2-4.

Figure 2-4 Riley Air Link (70°C Activation) Activated (left) and Un-activated (right)

2.4.2 Globe Technologies-Type A (57°C Activation)

The Globe Technologies Link is a two part fusible link, made of two similar semi-circle brass pieces. The two pieces are slightly different. One piece has an extruded part that fits into a rectangular hole on the other brass piece. Solder is put in between these brass pieces holding the link together. The link's surface is a shiny brass. This link is rated for a maximum load of 20.41 kg and a minimum load of 1.36 kg. This link is UL listed. Specific link data can be seen in Table 2-1 and a photo of the Model A Globe Technologies link activated (left) and un-activated (right) can be seen in Figure 2-5.

Figure 2-5 Globe Technologies Model A Link (57°C Activation) Activated (left) and Un-activated (right)

2.4.3 Globe Technologies-Type K (57˚C Activation)

The Globe Technologies Link Type K is similar in geometry to the Riley Air Link. Like the Globe Technologies Type A link, the plate has an extruded part that fits into the other piece of the link. The two pieces are identical, unlike the Type A link. The Globe Technologies Type K link plates are made of bronze instead of brass, unlike the Riley Air link and Globe Technologies Type A link. The two plates are held together by a solder with a melting temperature of 57˚C. The link's surface is shiny. This link is rated for a maximum load of 22.68 kg and a minimum load of 1.36 kg. This link is UL listed. Specific link data can be seen in Table 2-1. Figure 2-6 depicts the Model K Globe Technologies Link activated (left) and un-activated (right).

Figure 2-6 Globe Technologies Model K Link (57°C Activation) Activated (left) and Un-activated (right)

Link Data			
	Riley Air Link 70°C	**Globe Technologies 57°C Link**	**Globe Technologies 70˚C Link**
Length	0.06 (m)	0.0359 (m)	0.06 (m)
Width	0.016 (m)	0.0215 (m)	0.0194 (m)
Thickness	.0017 (m)	0.00363 (m)	0.00244 (m)
Mass	.0176 (kg)	0.0121 (kg)	0.0154 (kg)
Surface Area full frontal exposure	0.00096 (m^2)	0.0008 (m^2)	0.001 (m^2)
Surface Area worst possible exposure	.0001 (m^2)	0.0001 (m^2)	.0001 (m^2)
Volume	1.63 x 10^{-6} (m^3)	2.8 x 10^6 (m^3)	2.46 x 10-6 (m^3)
Density	10784.3 (kg/m^3)	4318.63 (kg/m^3)	6260.16 (kg/m^3)
Approximated Emissivity (Incorpera, 2005)	~0.6	~0.4	~0.4

Table 2-1 Specific Link Data Initial Conditions

3 Methodology

The objective of this report was to find a means of automatically closing a fire door or shutter before tempered glass window failure when exposed to a wildfire. The first step in addressing this issue was to consider a number of potential solutions developed using the design process shown (Norton, 2004):

- Identification of Need
- Background Research
- Goal Statement
- Performance Specifications
- Ideation and Invention
- Analysis
- Selection
- Detailed Design

In the end of this process it was deduced that fusible links were potentially the most feasible solution. In order to verify the use of fusible links in this application experimental testing was done. This experiment used a gas fired radiant panel array in combination with a movable test rig capable of simulating actual wildfire conditions, as done in the Bushfire CRC report discussed in Section 2.1. The results from the experimental testing were then verified with the calculated results of a thermal response model similar to the three-parameter model discussed in Section 2.3.3. The experimental results and simulated results generated by the thermal response model were then used in combination with existing literature on window failure to verify the use of fusible links in wildfire applications.

3.1 Experimental Procedure

3.1.1 Laboratory setup

Gas-fired Radiant Panel Array Testing

To simulate wildfire conditions, a gas-fired radiant panel array test apparatus at the CSIRO–Highett site was used. This is the same apparatus that was used in the experimental testing of the Bushfire CRC report. The test apparatus consists of a gas-fired radiant panel with a trolley on a track perpendicular to the center line of the panel. The gas-fired radiant panel array is 1500 mm by 1500 mm. Each individual panel on the

array is 137 mm by 137 mm. The panel is capable of producing radiation values of up to approximately 80 kW/m^2 (CRC, 2005). Liquefied Petroleum Gas (LPG) is used in the test apparatus. Two 200 liter tanks used as containers for the apparatus, shown in Figure 3-1, these tanks are kept outside of the laboratory for safety purposes.

Figure 3-1 LPG Gas Containers Used with Radiant Panel Array

For experiments test specimens were mounted on the trolley and pulled towards the gas-fired radiant panel array, shown in Figure 3-2 and Figure 3-3. The trolley was connected to a draw wire linear displacement transducer to measure its displacement (CRC, 2005). Movement of the trolley is computer controlled allowing for multiple tests under the same conditions. The control program (RPcontrol) is run through Microsoft excel where each line of the program gives a displacement and a number of seconds to stay at that displacement. It is possible to simulate various radiation profiles with this setup.

Figure 3-2 Test Rig in Operation (1)

Figure 3-3 Test Rig in Operation (2)

The computer is also used for data acquisition. Data is recorded in time-step intervals of one second. Thermal radiation exposures, front and back surface temperatures of links, ambient temperature of the room, convective cooling airflow temperature and ambient temperature at the links was all recorded by the computer. Data files produced are accessible through Microsoft Excel. Each experiment was videotaped, with the camera setup adjacent to the radiant panel to monitor the specimens through the entire

experiment and to protect the camera and operator from dangerous heat fluxes, as shown in Figure 3-2.

Fusible link test rig setup

The set-up for the experiment was arranged such that two specimens could be tested in each trial. Cement board (1.20 m by 1.48 m) was attached to the trolley parallel to the radiant panel array to simulate a building wall. An L-bracket metal frame attached to the water cooled frame of the trolley. The arm of the L-bracket extended 0.405 m away from the cement board. Metal wire was attached to the top bracket of the frame to hang the test specimens from. The metal wire holding the test specimens was secured by U-bolt wire clamps. Ten kilogram weights were attached to the bottom of each specimen by metal wire. The metal wire connecting the specimen and weight was strung through the bottom bracket of the metal frame to reduce movement of the specimen during tests. The bottom wire length was long enough so when the fusible link activated the weight would hit the floor and not pull on the frame. It was also short enough so the weight would get pulled by the trolley before hitting the body of the trolley. This was necessary for testing two links with the possibility of different activation times. This experimental set up is depicted in Figure 3-4 and Figure 3-5.

Figure 3-4 Experimental Test Set Up of Test Rig (Side View)
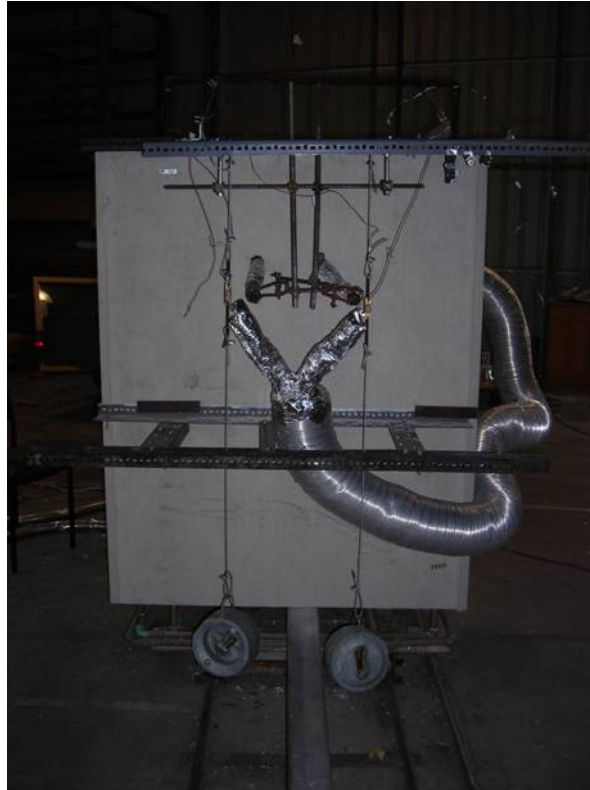
Figure 3-5 Experimental Test Set Up of Test Rig (Front View)

Convective cooling to the links was supplied by a centrifuge fan mounted at the rear of the trolley behind the cement board, shown in Figure 3-5. The fan exhaust was ducted to the links using flexing tubing. A split in the duct was made before reaching the links on the front side of the test rig allowing more direct airflow over the specimen. Each duct was oriented to allow airflow over both sides of the specimen for maximum convective cooling, as shown in Figure 3-5.

Radiometers were mounted adjacent to each specimen to get an accurate measurement of what radiation level that each specimen was exposed to. Bare wire thermocouples were mounted on the front and back face of each specimen. The bare wire thermocouples were held in place by bending the thermocouple wire such that the pressure of the wire held itself against the face of the specimen. The thermocouple wires were taped to the metal wires holding the specimen to secure the thermocouple during testing. A MIMS thermocouple was also mounted inside of the air duct near the exhaust exit to monitor the

temperature of the air across the specimens. An aspirated MIMS thermocouple was mounted in between the two specimens to monitor the ambient temperature the links were exposed to.

Activation Temperature Testing

The activation temperature of each link was specified by the manufacturer. This specification is often engraved on the fusible link. This can be seen in Figure 2-5 and Figure 2-6. Experimental testing was done to verify these specified activation temperature ratings. This was done using a bath of water in which the fusible link was submerged. Weights of 10 kg were also submerged and acted as an applied load for the submerged link. The bath of water was gradually heated in approximately 1˚C increments and the links were submerged for approximately 60 seconds for each temperature increment. This procedure was repeated until link activation. The temperature at which the link activated was then considered the activation temperature of the link.

Change of Phase Testing

To measure the specific Change of Phase (CHP) parameter for the different types of specimens a Weiss-Gallenkamp electric oven shown in Figure 3-6 was used to heat the specimens. The Weiss-Gallenkamp oven had a range of thirty to two hundred degrees Celsius (°C) and could be adjusted in increments of one-degree Celsius. The temperature of the oven was set to a temperature fifteen degrees higher than the specified activation temperature of the links.

Figure 3-6 Weiss-Gallenkamp Electric Oven

Given the nature of the CHP parameter, any temperature above activation temperature of the specimen can be used as it is a comparison of the areas under the curves as discussed in Section 2.3.3. The oven had a three and a half centimeter hole in the roof of the oven. Each specimen was hung in the oven by metal wire attached to a metal bar on the top of the oven; this experimental set up inside the oven is shown in Figure 3-7. A ten kilogram weight was attached to the bottom of each specimen by metal wire. Padding was placed in the bottom of the oven to prevent damage from the ten kilogram weight to the oven after activation.

Figure 3-7: CHP Experimental Set Up Inside Oven

To measure the solder temperature of each specimen a hole was drilled into the solder of the specimen and a bare wire thermocouple was inserted into the hole, as shown in Figure 3-8. The hole was filled with thermal paste before inserting the thermocouple. A type K mineral-insulated metal sheath (MIMS) thermocouple was used to measure the ambient temperature within the oven.
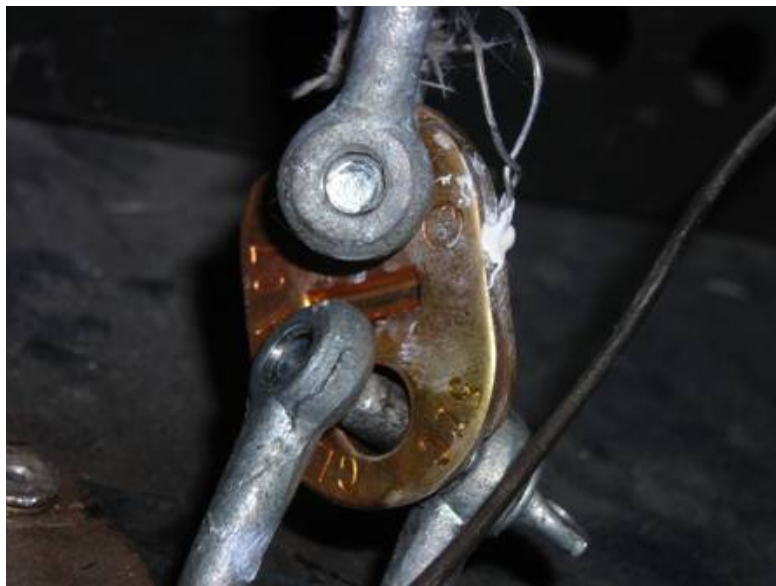
Figure 3-8 CHP Experimental Set-Up Thermocouple Mounting

To acquire data, thermocouples were attached to a DT800 dataTaker. The computer program DeTransfer was used to write a program to talk to the dataTaker and record data, this data acquisition setup is shown in Figure 3-9. Data files were accessible through Microsoft Excel.
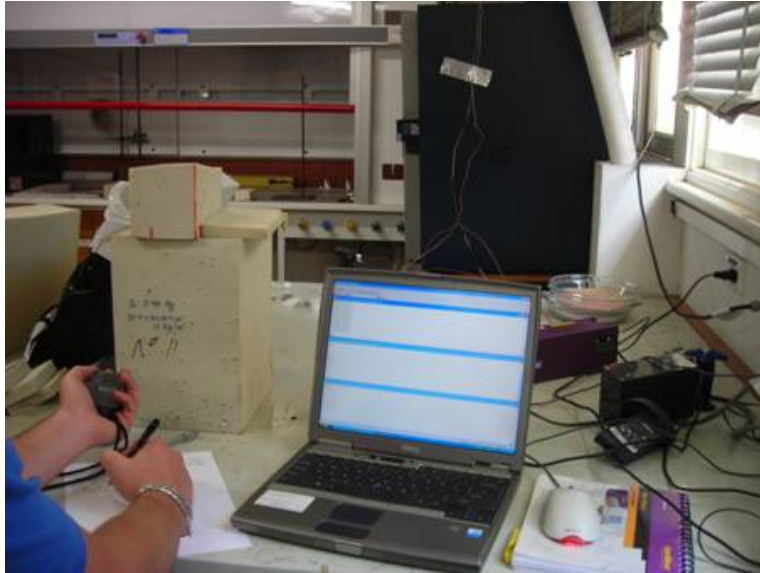
Figure 3-9 CHP Data Acquisition Set-Up

Conductance Testing

In order to determine the conductance of the fusible link and associated attachments, the two parameter method used by Heskestad and Bill discussed in Section 2.3.2 was used. Solving for the conductance required results of two different experiments; a plunge test and a ramp test. Together the results of the experiments can be used to create a system of equations, consisting of Equation (8) and Equation (13).This system is used to solve for the two unknowns, conductivity (C) and Response Time Index (RTI). After solving for C and RTI the conductance (C') parameter was solved using Equation (14). In both the plunge test and the ramp test experiments a test rig was set up in which the links were mounted in tension with accessories used to simulate actual conditions, this is shown in Figure 3-10.

Figure 3-10 Test Rig Used in Plunge and Ramp Tests

Ramp Test

The ramp test was done with existing equipment located on the CSIRO-Highett facility, the apparatus used is shown in Figure 3-11. Typically, this machine is used to determine the activation time of heat detectors; it normally operates with a known rate of temperature rise which is calibrated daily. The test apparatus is equipped with two calibrated bare wire thermocouples which sense the temperature of the air flowing within the oven's loop and another thermocouple to measure the ambient temperature of the room. The room is temperature controlled with an independent heating and air conditioning system. A baffle/screen is mounted within the oven's loop to create a uniform flow within the loop. The oven is heated by three computer-controlled electric heaters, located in the bottom left of the oven's loop, shown in Figure 3-10.

Figure 3-11 Plunge Test and Ramp Test Apparatus

In the ramp test the temperature of the ambient conditions are recorded, as well as the rate of rise, oven temperature at link activation and the experimental time of activation. This ramp test data, in combination empirical data from a plunge test was used to determine the conductance parameter (C').

Plunge Test

The same testing apparatus was used in order to run a plunge test. A plunge test, discussed in Section 2.3.1 is a test in which the temperature of the air within an oven is maintained at a constant temperature and the airflow within the oven is constant and uniformly distributed. In order to calibrate the existing testing apparatus capable of a plunge test modifications to the apparatus were required. The three electric heaters in the oven were normally controlled (in the ramp test configuration) by a frequency drive interfaced with a computer. This configuration controls the rate of temperature rise in the apparatus's normal configuration. In order to operate the oven at a constant temperature in the existing apparatus at CSIRO it was necessary to bypass the existing system's frequency drive. This was done using an AC to DC converter and wiring the direct current directly to the electric heaters, this configuration is shown in Figure 3-12.By

modifying the equipment as such the oven would operate at a constant temperature which could be manually controlled by the constant DC input to the electric heaters.

Figure 3-12 Plunge Test Control System (AC to DC Converter)

As done in the case of the ramp test, the ambient conditions were recorded as was the temperature of the oven, the velocity of the air within the oven and the time at which the link activated. Together with the empirical data obtained from the ramp test, a system of equations was used to determine the Response Time Index (RTI) and the conductivity (C) of the fusible link and associated attachments. The conductance (C') was then solved using Equation (14)

Thermal Creep Testing

In order to test for thermal creep, it was necessary to have a raised temperature over a long period of time. To test for the potential of thermal creep a Weiss-Gallenkamp oven was used, depicted in Figure 3-6. The same specimen setup for the CHP test was used, and is depicted in Figure 3-7. The top of the specimen was attached by metal wire to a metal bar on top of the oven. A ten kilogram weight was attached to the bottom of the specimen with metal wire. Temperature in the oven was set at 50°C and left over a period of three days to simulate worst case scenario presented by an Australian summer.

To measure creep the original positions of the two plates in relation to each other were marked with permanent marker. The length of the specimen was measured before and after the test with Calipers. The links were tested over a period of three days and the length of each specimen was measured three times on a daily basis.

3.1.2 Testing Procedures

Radiative Panel Test Procedure

- Place radiation shield in front of test rig
- Mount specimens in rig. Attach top wire then bottom wire
- Adjust specimen to proper orientation for experiment
- Turn on centrifuge fan
- Adjust ducting so airflow is consistent over both faces of specimens
- Measure and record air speeds at location of each specimen
- Mount bare wire thermocouples to each specimen
- Turn on pumps for radiometers, test apparatus frame, and aspirated thermocouple
- Turn on Gas-fired radiant panel array
- Start data acquisition program
- When panel temperature is steady start recording video
- Remove radiation shield
- Begin radiation profile control program
- Record start of control program
- Record activation time of each specimen
- Shut off radiant panel and video recorder
- Stop data acquisition program
- Return trolley to starting position
- Replace radiation shield
- Shut off pumps and fan

Link Activation Temperature Test Procedure

- Fill a large bucket with cold water (a large bucket is used to minimize water currents).
- Heat the water in the bucket to 5°C below the manufacturer's specified activation temperature of the fusible link.
- Measure and record temperature.
- Insert fusible link (with 10 kg weight) into water.
- Gradually heat the water and monitor the temperature.
- Record the temperature at which the link activates.

Change of Phase Test Procedure

- Attach specimen to top wire, then attach bottom wire with weight.

- Pull specimen through hole in roof of oven and secure in place so specimen does not get conditioned when oven is pre-heating.
- Attach bare wire thermocouple to specimen
- Secure MIMS thermocouple inside oven
- Close and Turn on oven
- Begin data acquisition program
- When oven temperature stabilizes drop link into oven
- Mark down the time of the data acquisition program when link is submerged into the oven.
- Observe data to ensure that the bare wire thermocouple remained in the specimen
- Listen for weight hitting oven floor. Mark time of activation in data acquisition program
- Turn off oven
- Stop data acquisition program

Conductivity Test procedure

Ramp Test

- Attach specimen to the test rig. First to shackle then to turnbuckle
- Put specimen under tension by tightening turnbuckle
- Check data acquisition equipment to ensure that it will record the experiment
- Place specimen in sensitivity test rig and begin ramp test
- Start stop watch with beginning of test
- Observe specimen through window on test rig
- Flip the activation switch to stop data acquisition when specimen activates
- Test rig should automatically shut down, if not manually shut down
- Stop the stop-watch when specimen activates
- Record time to activation
- Print data sheet from acquisition computer
- Remove specimen from test rig
- Allow test rig to cool before performing the next experiment

Plunge Test

- Attach specimen to the test rig. First to shackle then to turnbuckle
- Put specimen under tension by tightening turnbuckle
- Check data acquisition equipment to ensure that it will record the experiment
- Configure sensitivity test rig reach equilibrium at a temperature above specimen activation temperature.
- Turn on sensitivity test rig and wait for temperature to level out
- Plunge test rig with specimen attached into the top of the sensitivity test rig
- Start stop watch
- Observe specimen through window
- When specimen activates stop the stop watch
- Record the activation time

- Record the air temperature within the sensitivity test rig
- Remove test rig and allow sensitivity test rig to cool down.

Thermal Creep Test Procedure

- Measure and record specimen length
- Mount specimen inside oven with metal wires.
- Place protective padding on oven floor
- Set oven temperature, close oven door, turn on oven
- Observe temperature rise to ensure oven temperature does not exceed activation temperature
- Leave specimen under load in raised temperature
- Periodically check specimen for signs of creep
- Measure specimen length every hour.

3.2 Calculated Modeling of Fusible Links

A thermal model of each fusible links was created. The thermal response model assumed that the link heated isothermally; therefore a lumped heat capacity was assumed. The model accounted for convective cooling, conductive losses to supporting structures, radiation losses, energy required for eutectic phase transformations and incident radiation fluxes. In accounting for conduction and change of phase energy additional experimental data was required to create the response model; this data was obtained by the methods discussed in Section 3.1.1 and Section 3.1.2.

In the model, the temperature profile of each link was calculated using the fourth order Runge-Kutta numerical method (Ross, 1989). The results of the model were later verified by experimental results. The basic heat balance equation used to create the model is shown in Equation (17). The individual components of Equation (17) are discussed and justified in the proceeding sections.

$$\rho V c_p \frac{dT}{dt} = A\varepsilon \cdot [\text{Incident Raditation}](X) - 2hA(T_E - T_\infty)$$

$$- [A\varepsilon\sigma T_s^4 - A\varepsilon\sigma T_\infty^4] - C'(T_E - T_o)$$

$$\rho V c_p \frac{dT_E}{dt} = \text{Energy Storage}$$

$$A\varepsilon \cdot [\text{Incident Radiation}] = \text{Incident Radiation}$$

$$(X) = \text{Fraction of Energy required by heat of fusion}$$

$$-2hA(T_E - T_\infty) = \text{Convective cooling (on 2 faces)}$$

$$-[A\varepsilon\sigma T_E^4 - A\varepsilon\sigma T_\infty^4] = \text{Radiative Losses}$$

$$- C'(T_E - T_o) = \text{Conductive Losses}$$

(17)

The use of the lumped heat capacity model was verified by the calculation of the Biot number, Equation (18) (Incorpera, 2005). Under this specification it is acceptable to assume that the solid is heated isothermally, due to small temperature gradients within the

link. As a result it is acceptable to assume a uniform temperature distribution within the element (Incorpera, 2005), this assumption is referred to as a lumped heat capacity.

$$Bi = \frac{hL_c}{k} < .1$$

L_c = Characteristic Length (V/A_s) (m)   (18)

k = Thermal Conductivity $(W/m \cdot {}^o C)$

h = Convection Coefficient $(W/m^2 \cdot {}^c C)$

3.2.1 Incident Radiation

In wildfires, radiation is the dominant mode of heat transfer. The incident radiation acting of the link is accounted for in the model by the term *"Incident Radiation"* in Equation (17). This *"Incident Radiation"* term represents the equation of a line which was fit to experimentally measured radiation profiles produced by the radiant panel and test rig, discussed in Section 4.1. The radiation profiles provided by the panel and test rig were selected to represent simulation of actual wildfire conditions as discussed in Section 2.1.

By fitting an equation to the radiation profile of the radiant panel and test rig data it ensures that the thermal response model is validating the actual experimental conditions. In some cases multiple curves, over varying time intervals were required to be fit to ensure the accuracy of the model.

3.2.2 Convective Cooling

In wildfire scenarios the potential for convective cooling of the links exists. This phenomenon can be caused by natural air currents or the flow of air entrained by the wildfire. This factor was accounted for experimentally by blowing ambient air over two faces of the links. This essentially simulates the worst case scenario in which both faces of a link would be cooled. As depicted in Figure 3-5, air does not exactly flow over the two faces as desired, however in calculations it was assumed that air passed over both sides of the link in cases where the link was fully exposed. In cases were the link was

mounted with the worst view factor it was assumed that air was incident on only one face of the link and this is accounted for in the calculations. A sensitivity analysis of convective cooling was performed, as seen in Section 4.7, based on these results potential errors attributed to the assumption of flow over the links was negligible.

The wind speeds chosen for the experimental evaluation were based on the wind speeds measured in the International Crown Fire Modeling Experiment. From the empirical data presented in the literature it was clear that wind speeds varied between 2.5 m/s and 4.4 m/s (Poon, 2002). These measurements were observed at 10 m and do no accurately represent the wind speeds present in Australia. Using the database put together by the Australian Bureau of Meteorology it was determined that a mean wind speed at 1.2 m in height was approximately 6.5 m/s, this data is based on 37 years of data (Bureau of Meteorology, 2007), this data was taken for the Highett area. The wind speed presented by the Bureau of Meteorology are an average measurement of wind speeds, consequently this measurement does not account for circumstances high wind speeds.

Using the McArthur Forest Fire Danger Meter Mk5 to compute the Fire Danger Indicator (FDI) it was found in order to achieve conditions where 40 kW/m^2 radiant exposures exist the ambient temperature would need to be 30˚C with high wind speeds of 25 m/s at heights of 10 m above the ground (Webb, 2007). The wind speed at the ground level in a treed environment is generally determined to be 1/3 of the wind speed measured at a 10 m elevation. As a result wind speeds can reach up to approximately 8 m/s (Webb, 2007).

Therefore, the range of experimental velocities used varied between approximately 4 m/s and 8 m/s. The wind speeds used in the experimental testing were not a major consideration in the report because the range of potential wind speeds passing over the fusible links resulted in Reynold's Numbers indicating a laminar flow. Based on this the constructed thermal response model would be capable of accounting for an even wider range of wind speeds than those tested experimentally.

Convective cooling was accounted for in the thermal response model by the "$-2hA(T_E - T_\infty)$" term used in Equation (17). The value of convective heat transfer coefficient (h) is a function of the wind speed passing over the link and was calculated using Equation (19), Equation (20) and Equation (21). The variable in these calculations was the wind speed, the input of this variable depended on the measured wind speed of the particular experiment used to validate the model. The experimentally simulated wind speeds were measured, as shown in Figure 3-13 using the calibrated meter shown in Figure 3-13

Figure 3-13 Measuring Simulated Wind Speeds

Figure 3-14 Handheld Anemometer used for Velocity Measurements

There were a series of three steps necessary to calculate the convective heat transfer coefficient (*h*) which included the calculation of the Reynolds Number (19) and the calculation of the Nusselt Number (20) (Incorpera, 2005).

$$\text{Re}_D = \frac{\mu \cdot D}{\nu}$$

$\mu = WindSpeed(m/s)$
$D = PlateThickness(m)$ (19)
$\nu = KinematicVis\cos ity(m^2/s)$

It was assumed that the the cooling air passed over a flat plate, this assumption was made to simulate the worst case scenario. The characteristic length in the case of flow over a flat plate is the ratio of the volume of each link respectively to the area of the link (Incorpera, 2005) (Kozanoglu, 2006). Essentially this dimension is approximately the thickness of the plate, but due to holes in each link the characteristic lengths are not exactly the thickness of the given link.

In calculating the Nusselt Number it was assumed that the wind was passing over a vertical plate. Traditionally, Nusselt Number calculations calculate the dimensionless number representing the ratio of convective to pure conduction heat transfer for flow over circular elements (Incorpera, 2005). However, it is possible to calculate the Nusselt number when passing over a non-circular element by multiplying by an established correction factor (Incorpera, 2005). As a result, Equation (20) is required to calculate the Nusselt number for a flow passing over a vertical plate, correction factors for flow over a flat plate are indicated below Equation (20).

$$\overline{Nu}_D = C \cdot Re_D^m \cdot Pr^{1/3}$$

$$
\begin{array}{l}
C = .228 \\
Re_D = \text{Reynolds Number} \\
m = .731 \\
Pr = \text{Prandtl Number}
\end{array}
$$

(20)

After determining the Reynolds Number and the Nusselt Number, the convective heat transfer coefficient (*h*) was calculated using Equation (21). After determining the convection coefficient (*h)* the convective losses were accounted for by inserting the value of *h* into Equation (17).

$$\overline{h} = \overline{Nu}_D \cdot \left(\frac{k}{D}\right)$$

$$
\begin{array}{l}
\overline{Nu}_D = \text{Nusselt Number} \\
k = \text{Conductivity } \left(\frac{W}{m \cdot {}^o C}\right) \\
D = \text{Plate Thickness (m)}
\end{array}
$$

(21)

3.2.3 Radiative Cooling

In accounting for radiation losses from the link Equation (22) was used, because the thermal response model is transient the value of T_E increases with time, thereby adequately accounting for the rise of temperature of the link and consequently greater

radiation losses from the link to the surrounding air. In the thermal response model calculations the temperature of the ambient air is assumed to be fixed.

$$\text{Radiant Losses} = -(\varepsilon_{link}\sigma A T_E^4 - \varepsilon_{air}\sigma A T_\infty^4)$$

$$
\begin{aligned}
\varepsilon_{link} &= \text{Emissivity of Link} \\
\varepsilon_{air} &= \text{Emissivity of Air} \\
\sigma &= 5.67\text{x}10^{-8}\left(W\big/m^2 \cdot {}^o C^4\right) \\
A &= \text{Surface Area of entire link (all sides) (m}^2) \\
T_E &= \text{Link Temperature } ({}^o C) \\
T_\infty &= \text{Ambient Temperature } ({}^o C)
\end{aligned}
\tag{22}
$$

3.2.4 Conduction Losses

In accounting for the conductive losses the two-parameter model discussed in Section 2.3.2 and Section 3.2.4 was used. A plunge test and a ramp test were used to create a system of two equations; Equation (8) and Equation (13). Upon determining these values for conductivity (C) and Response Time Index (RTI) the conductance parameter (C') was determined using Equation (14). The value of C' was inserted into Equation (17) thereby accounting for conduction losses from the heat sensitive element to the link and the link connections.

3.2.5 Runge-Kutta Numerical Method

The differential equations in the model were solved using the 4th order Runge-Kutta numerical method. In this approximation values for k1, k2, k3 and k4 were determined using a time step of 1 second intervals, as seen in Equation (23) (Ross, 1989). After computing the intermediate "k values" the temperature at each particular time was computer using Equation (24) (Ross, 1989).

$$k1 = \Delta t \cdot f(t,T)$$

$$k2 = \Delta t \cdot f(t + \frac{\Delta t}{2}, T + \frac{k1}{2})$$

$$k3 = \Delta t \cdot f(t + \frac{\Delta t}{2}, T + \frac{k2}{2})$$

$$k4 = \Delta t \cdot f(t + \Delta t, T + k3)$$

(23)

$$T_E = \frac{k1 + 2 \cdot k2 + 2 \cdot k3 + k4}{6} + T_o$$

(24)

3.2.6 Model Verification

In order to verify the model, experimental results were compared with calculated results. This comparison was done qualitatively and quantitatively. A qualitative assessment included comparing graphically plotted time temperature profiles from experimental and calculated results. The quantitative assessment used the R-Squared method which is used to indicate the predictive power of a given model (Draper and Smith, 1981). Equation (25) is used to calculate the R-Squared value.

$$R^2 = \frac{\sum(\hat{Y}_i - \bar{Y})^2}{\sum(Y_i - \bar{Y})^2}$$

(25)

R^2 = Coefficient of multiple determination

$\hat{Y}_i$ = Predicted value from model

$\bar{Y}$ = Mean value

Y_i = Observed value

The experimental data selected for comparison to the model pertained to links with the known variables. In this case all links were painted black with radiometer paint. As a result the emissivity of the links could be assumed to be approximately $\varepsilon=0.9$, as indicated by the paint specifications.

As a general guide R^2 values greater than 0.8 indicate a feasible model, whereas R^2 values less than 0.8 would indicate that the model's predictive powers were questionable.

This general guideline was used to evaluate the modeled radiation equations which were based on empirical data and then again in the evaluation of the validity of the thermal response model.

4 Findings and Results

In this section the results from the experimental testing are shown. Because a number of different types of tests have been performed, the results have been broken up into distinct sections. The results include the experimentally determined minor effect of conductance, the significant role or energy required by the heat of fusion, and most importantly the link activation times when the links were mounted in best and worst case scenarios as well as best and worst case emissivity.

4.1 Gas-Fired Radiant Panel Array Test

4.1.1 Radiation Profile Exposures

To calibrate the radiative panel array and test rig, an experiment was conducted without test specimens (fusible links). Data was recorded with mounted radiometers and then compared to the radiation profiles used in the Bushfire CRC report, discussed in Section 2.1. Adjustments were continually made in the test rig's operation to ensure that the experimental radiation profile used in actual testing accurately matched the profiles used in the Bushfire CRC report, depicted in Figure 2-2. An example of these experimental results versus the Bushfire CRC radiation profile used is shown in Figure 4-1.
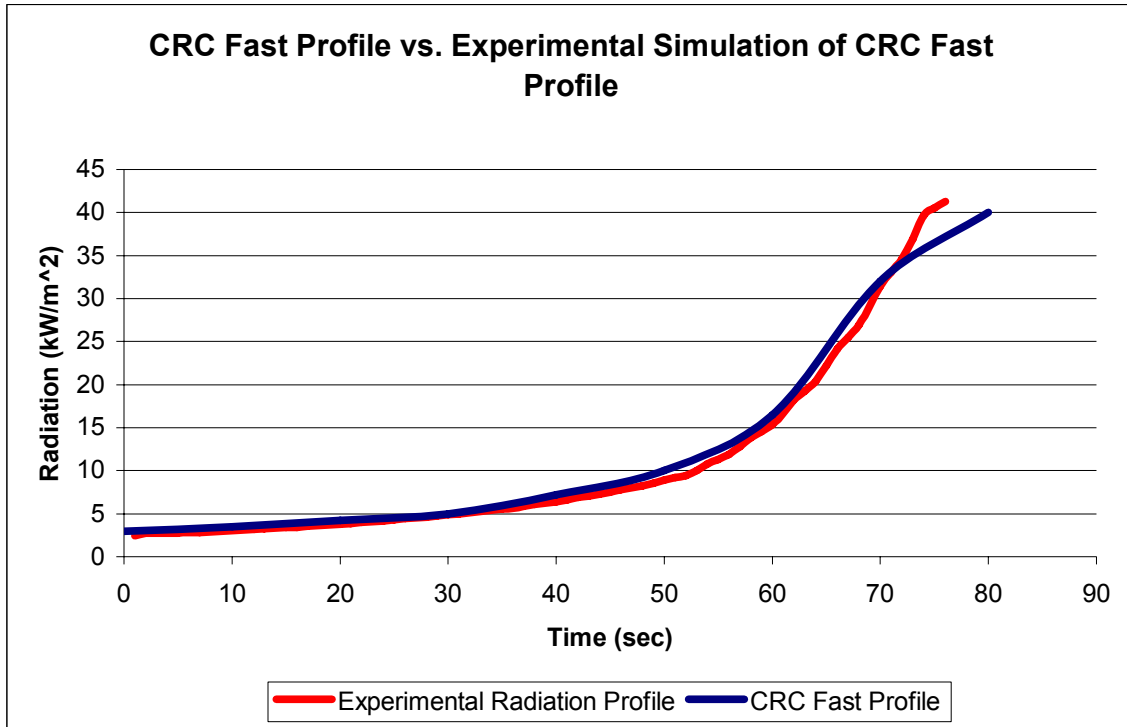
Figure 4-1 CRC Fast Profile vs. Experimental Fast Profile

4.1.2 Link Activation Testing

As discussed in Section 3.1, three different fusible links were tested. A number of different link configurations (view factors) were tested as well as links with altered emissivities. Testing done on the unaltered links exposed to the fast radiation profile resulted in different activation times for each type of link as indicated in Table 4-1. Similarly results for each link exposed to the slow profile are shown in Table 4-2.

Fast Profile - Unaltered Links			
	Mean (seconds)	Standard Deviation	Number of Tests
Riley Air Link	92.5	±35.6	3
Globe Technologies Model A Link	112	±11.14	4
Globe Technologies Model K Link	N/A	N/A	N/A

Table 4-1 Activation Times of Each Unaltered Link Exposed to Fast Profile

Slow Profile – Unaltered Links			
	Mean (seconds)	Standard Deviation	Number of Tests
Riley Air Link	574	±4.2	2
Globe Technologies Model A Link	610	±4.2	4
Globe Technologies Model K Link	N/A	N/A	N/A

Table 4-2 Activation Times of Each Unaltered Link Exposed to Slow Profile

As mentioned links were also tested with an altered emissivity in both the slow and the fast radiation profiles discussed in Section 2.1, in altering the emissivity the links were painted black with radiometer paint with a manufacturer specified emissivity ($\varepsilon = \sim 0.9$) as discussed in Section 3.1. The results from these tests are generalized in Table 4-3 and Table 4-4.

Fast Profile - Painted Links ($\varepsilon = \sim 0.9$)			
	Mean (seconds)	Standard Deviation	Number of Tests
Riley Air Link	68	±1.4	4
Globe Technologies Model A Link	65	±2.8	2
Globe Technologies Model K Link	72.5	±1.3	3

Table 4-3 Generalized Activation Results of Each Link ($\varepsilon = 0.92$) Exposed to Fast Profile

Slow Profile - Painted Links ($\varepsilon = \sim 0.9$)			
	Mean (seconds)	Standard Deviation	Number of Tests
Riley Air Link	392.5	±14.9	5
Globe Technologies Model A Link	366.5	±32.5	2
Globe Technologies Model K Link	358.8	±33.9	3

Table 4-4 Generalized Activation Results of Each Link ($\varepsilon = 0.92$) Exposed to Slow Profile

These results are discussed at length in Section 4.7, however based on the calculated standard deviations of the experimental results it is not possible to indicate which model fusible link has a faster activation time when exposed to simulated wildfire conditions. In order to determine which link has the fastest activation time it would be necessary to run

additional tests in order to prove a trend in the data. This was not done in this investigation for two primary reasons; the primary reason was because the goal of the project was to determine whether or not the fusible links would activate prior to window breakage and the reason for the limited number of tests was the limited supply of fusible links, and consequently the budget of the project.

The effect of each the emissivity parameter was evaluated in the experimental data and is discussed in the proceeding sections. Additionally the effect of view factor, explained in Section 4.1.4 is discussed in the proceeding sections.

4.1.3   Emissivity

The emissivity of fusible links was found to play a major role in the activation time of the links. The experimental data indicated that a rise in emissivity correlated to a faster activation time, as seen in Figure 4-2. This figure is a comparison of empirical data of Riley Air links exposed to the fast profile where the emissivities were unaltered ($\varepsilon = \sim 0.4$ to $\varepsilon = \sim 0.6$) and altered ($\varepsilon = \sim 0.9$). For the link with an emissivity of $\varepsilon = \sim 0.4$ to $\varepsilon = \sim 0.6$ the activation time was 95 seconds (24_01_07-test1) . For the link with an emissivity of $\varepsilon = \sim 0.9$ the activation time was 71 seconds (25_01_07-test1). This finding was seen throughout the experimental data in both the fast and slow profiles for all three types of fusible links tested in this report.
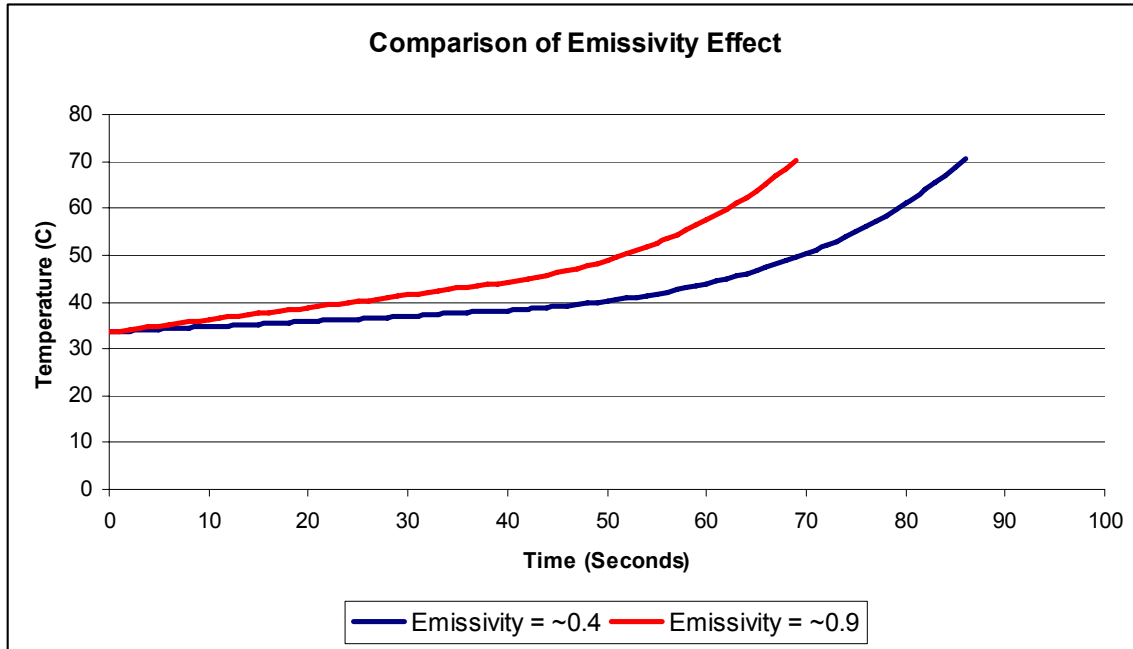
Figure 4-2 Globe Technologies Model K Link Fast Profile Comparison of Emissivity Effect

The Slow Profile for Riley Air Links showed the same experimental trend, this is seen in Figure 4-3 for the link with an emissivity of $\varepsilon= {\sim}0.4$ to $\varepsilon= {\sim}0.6$ the activation time was 577 seconds (25_01_07-test2), where the activation time for the link with an emissivity of $\varepsilon= {\sim}0.9$ was 460 seconds (25_01_07-test4). This is further support towards the finding that increased emissivity decreases activation times.
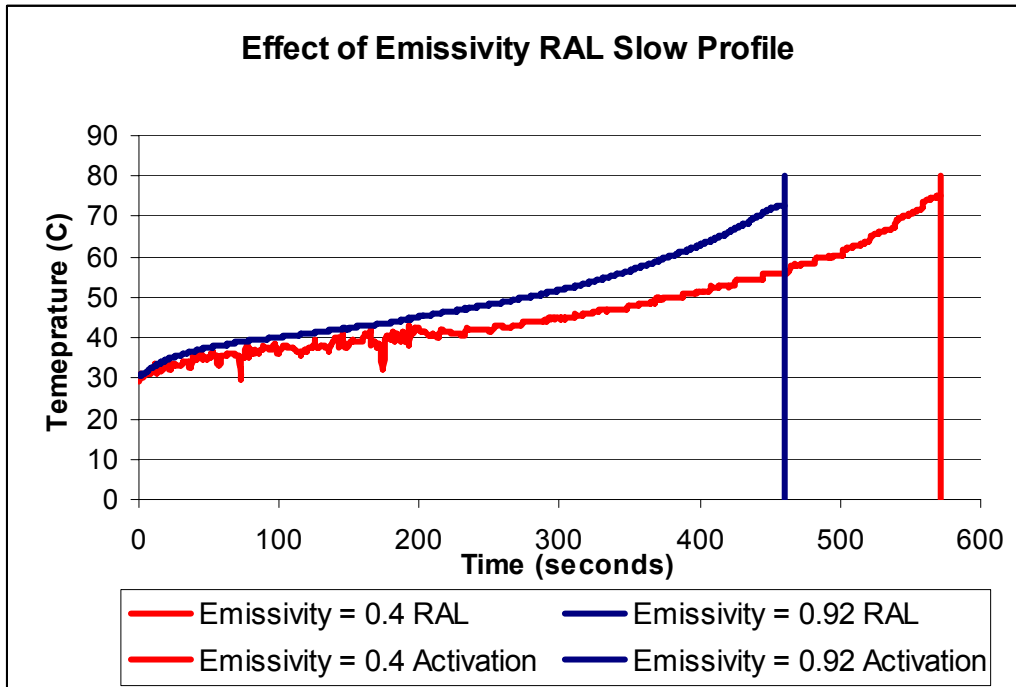
Figure 4-3 Riley Air Link Slow Profile Experimental Comparison of Emissivity Effect

4.1.4 View Factor

As done in the case of the effect of emissivity testing, when links were mounted with the worst case view factor it was found that activation times increased. This was found to be the case for all links and radiation profiles. An example of this result is shown by Figure 4-4. In this figure activation time where the Riley Air link was mounted in the worst possible configuration the activation time was 97 seconds, whereas for best case view factor activation time was 67 seconds.
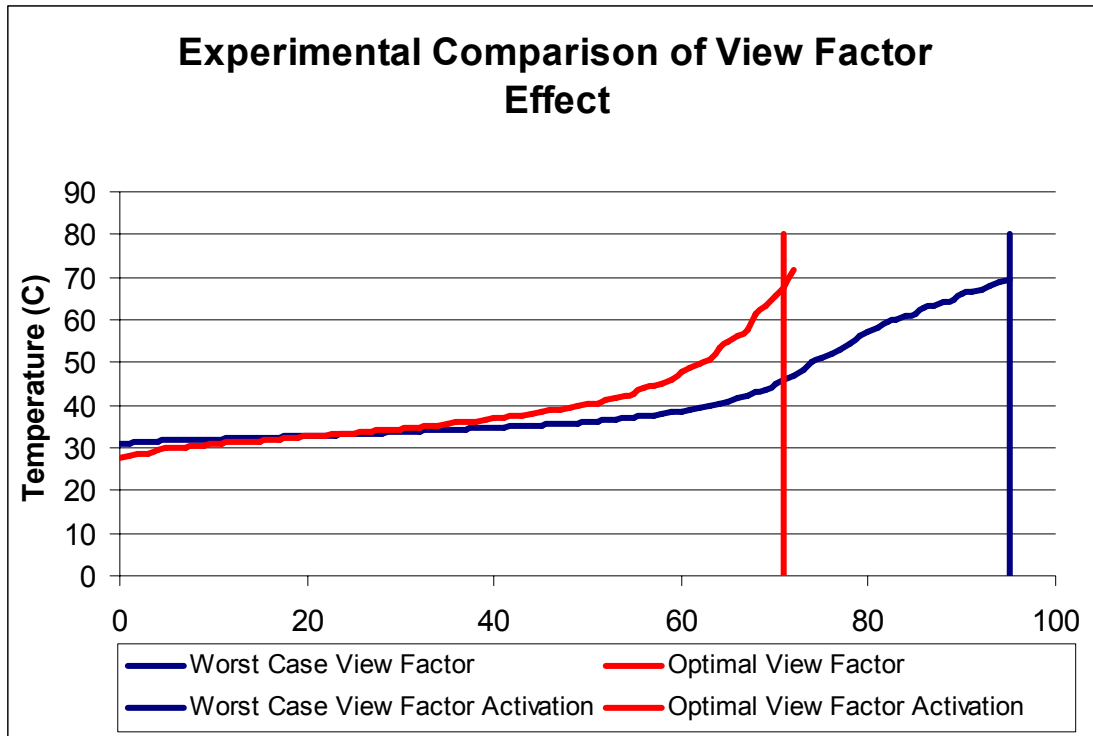
Figure 4-4 Riley Air Link Fast Profile Experimental Comparison of View Factor Effect

4.2 Change of Phase (CHP) Test

In order to determine the energy required for the solder of the fusible link to undergo a phase change the test method described in Section 3.1.1 and Section 3.1.2 was used. The results for each link type are discussed in the proceeding sections.

4.2.1 Riley Air Link (70˚C Activation)

It was not possible to determine the change of phase parameter. Multiple attempts to obtain experimental data resulted in inconsistent results. The reason for this inconsistency is due to the physical inability to measure the temperature of the link's solder. The construction of the Riley Air Link does not permit a thermocouple to be mounted in a configuration that the temperature of the solder could be measured. As a result experimental results measured the temperature of the brass of the fusible link, not the temperature of the solder. As a result of this the heat of fusion of the solder could not be calculated. Inputs into the thermal response model were based on estimations considering

the successfully obtained results from the Globe Technologies Model K and Model A links.

In testing for the heat of fusion energy for the Riley Air Link a mechanical problem with the link was discovered which affected the proper activation of the link. In one of the attempted tests the Riley Air Link had reached the activation temperature and the solder had melted to a point where the link *should have* activated, however the link failed to operate because the roller key of the fusible link prevented the two separated pieces of the link from detaching from one another.

Additional background investigation was done and it was determined that roller keys are often used in fusible links, however they are usually positioned perpendicular to the line of link activation, as depicted in Figure 4-5. Roller keys are used to aid in the separation of the links (Ierardi, 2007). In the case of the Riley Air Link, the roller key is positioned parallel to the line of link activation As a result of this design; the potential exists in which the roller key would prevent proper link activation.
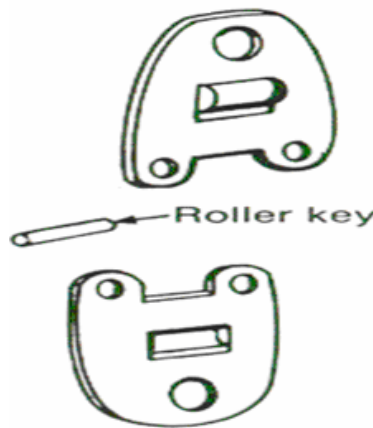
Figure 4-5 Typical Roller Key Configuration in Fusible Links

4.2.2   Globe Technologies Model K Link (57°C Activation)

The heat of fusion for the Globe Technologies Model K link was determined from the experimental procedure described in Section 3.1.1. The graphical results for this link can

be seen in Figure 4-6 and Figure 4-7. The vertical lines represent the time of phase change initiation and the time of link activation (respectively).

Microsoft Excel was used to fit curves using least squares approximations to provide equations for the empirical data. The curves of the oven temperature and solder temperature profiles (respectively) are listed on the side of each graph. Additionally the R^2 value of each fitted equation is listed, in each case the R^2 values indicate strength of the simulated equation. The areas A and B were determined using integral calculus, results are shown in Table 4-5 for the first test and Table 4-6 for the second test.
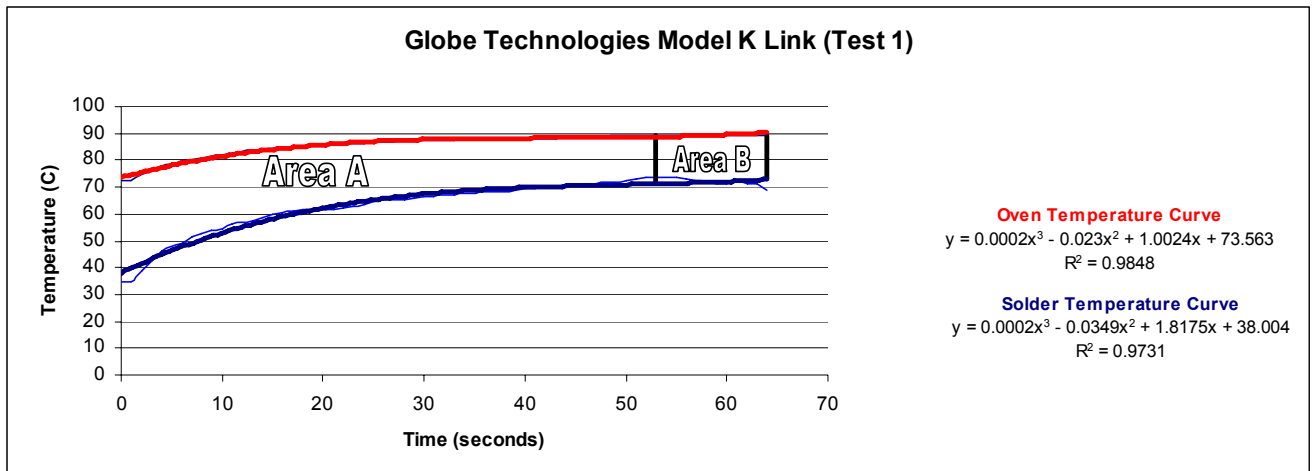
Figure 4-6: Globe Technologies Model K (Test 1) Graphical Results

Section	Calculated Area (Units^2)
Area A	1330.305429
Area B	315.8796541
Total Area	1646.185083

Table 4-5: Globe Technologies Model K (Test 1) Calculated Area Results

From these results it was determined using Equation (16) that the energy required to cause a phase change in the solder was 19%. This experimental result indicates that 81% of the incident radiation goes into heating the fusible link to the activation temperature. A second test was done to validate this finding and the results are shown in Figure 4-7. The calculated area results for these plots are shown in Table 4-6.
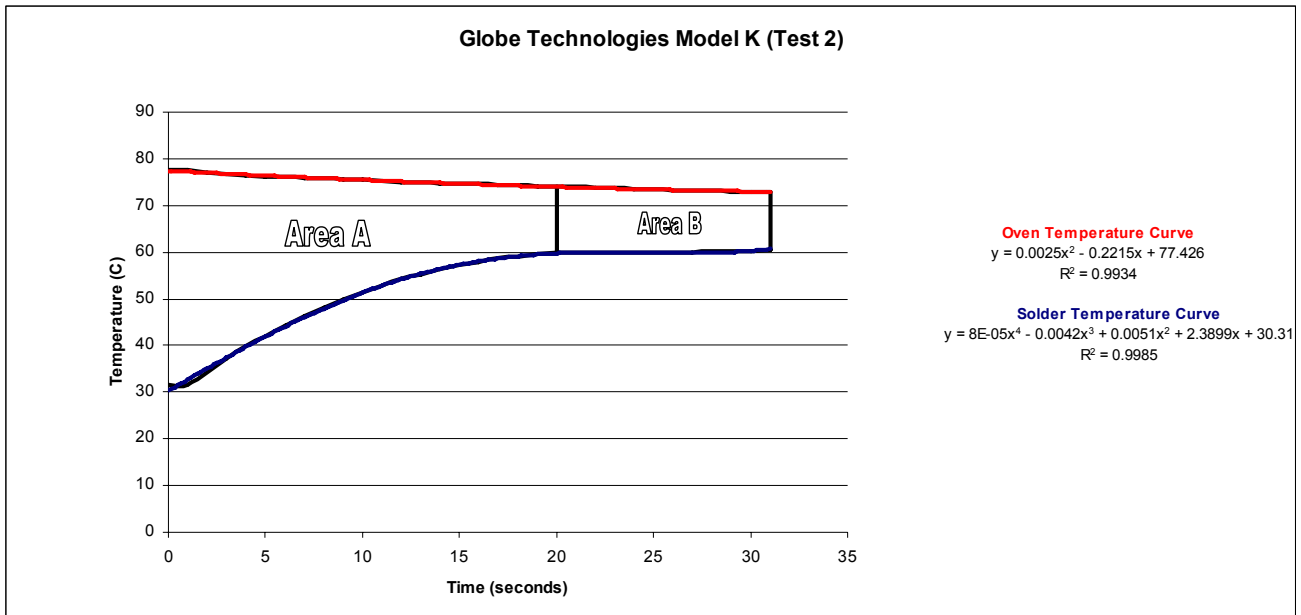
Figure 4-7: Globe Technologies Model K (Test 2) Graphical Results

Section	Calculated Area (Units^2)
Area A	529.9
Area B	161.7
Total Area	691.6

Table 4-6 Globe Technologies Model K (Test 2) Calculated Area Results

From these results it was determined using Equation (16) that the energy required to cause a phase change in the solder was 23%. This experimental result indicates that 77% of the incident radiation goes into heating the fusible link to the activation temperature.

4.2.3   Globe Technologies Model A Link (57˚C Activation)

As done with the Globe Technologies Model K Link, the areas respective areas of A and B were calculated to determine the fraction of the energy required to cause the phase change of the solder in the fusible link. This was done in two experiments whose results are depicted in Figure 4-8 and Figure 4-9. The calculated area results from Figure 3 can be seen in Table 3.
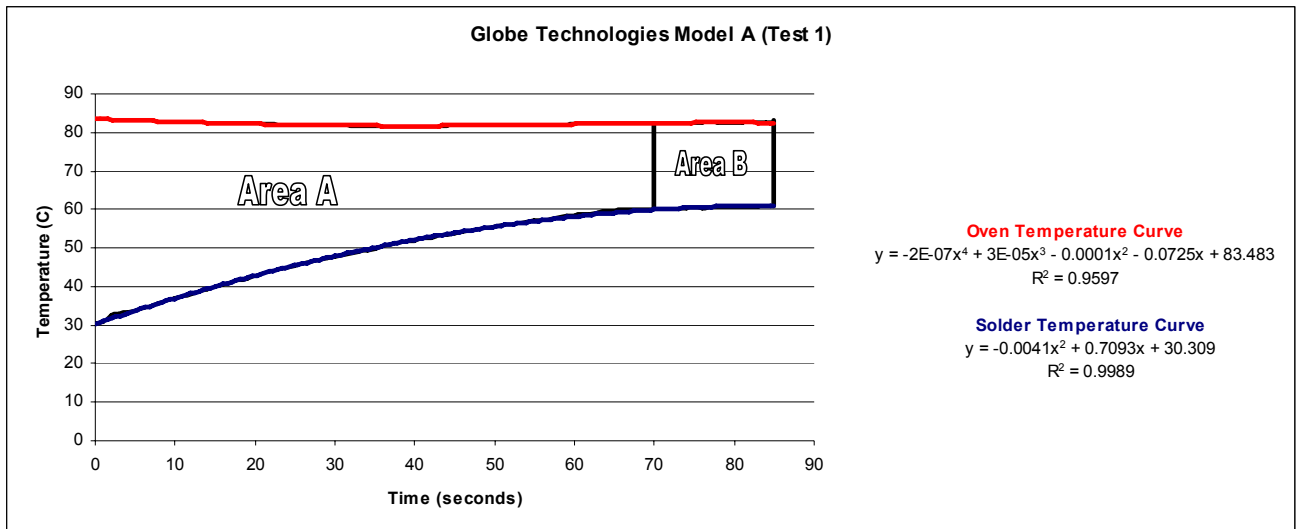
Figure 4-8: Globe Technologies Model A (Test 1) Graphical Results

Section	Calculated Area (Units^2)
Area A	2376.9
Area B	351.4
Total Area	2728.3

Table 4-7: Globe Technologies Model A (Test 1) Calculated Area Results

These results when inserted into Equation (16) and indicate that 13% of the total incident energy is required to cause the phase change of the solder. This infers that 87% of the total incident energy goes into heating the fusible link. A second test was done using the same link, whose results are depicted in Figure 4-9.
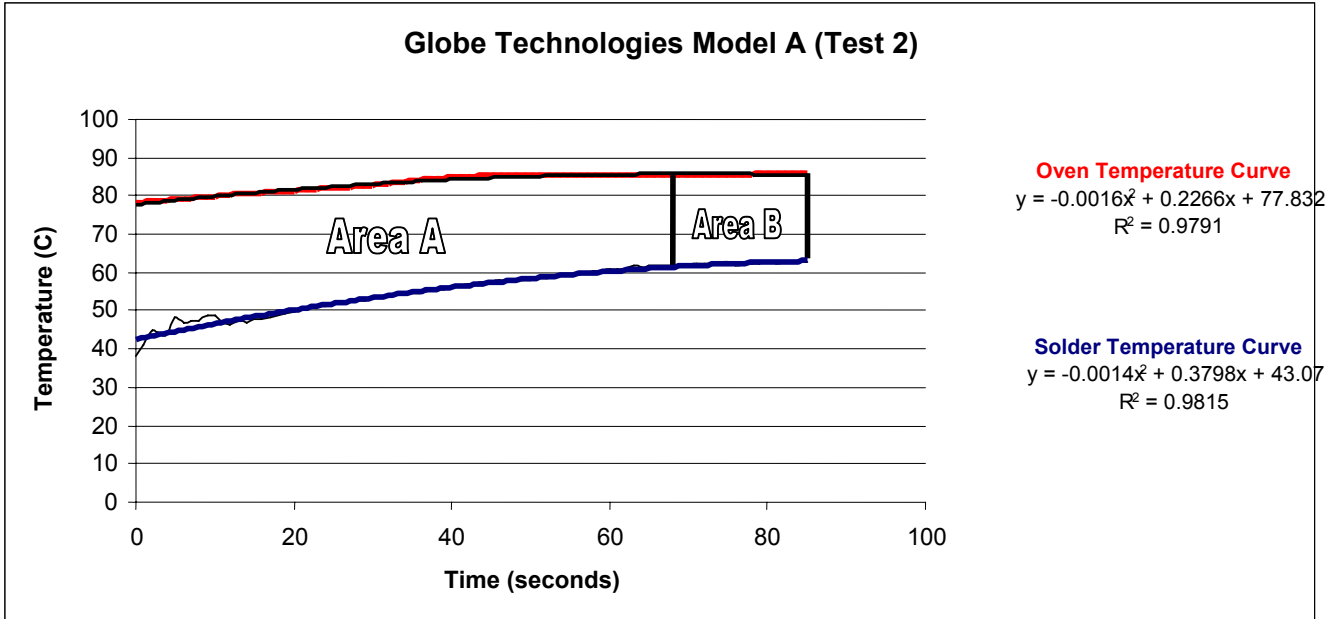
Globe Technologies Model A (Test 2)

Temperature (C)

Area A   Area B

Oven Temperature Curve
$y = -0.0016x^2 + 0.2266x + 77.832$
$R^2 = 0.9791$

Solder Temperature Curve
$y = -0.0014x^2 + 0.3798x + 43.07$
$R^2 = 0.9815$

Time (seconds)

Figure 4-9: Globe Technologies Model K (Test 2) Graphical Results

Section	Calculated Area (Units^2)
Area A	1988.7
Area B	371.7
Total Area	2360.4

Table 4-8: Globe Technologies Model A (Test 2) Calculated Area Results

From these results of Table 4-8 it was determined using Equation (16) that the energy required to cause a phase change in the solder was 16%. This experimental result indicates that 84% of the incident radiation goes into heating the fusible link to the activation temperature.

4.3 Link Activation Temperature Testing

The method and procedure described in Section 3.1 was used to determine the actual activation temperature of each fusible link. While each link is marked with the manufacturer's specified activation temperatures, testing was done to verify this. In the case of the Riley Air Link it was found that the activation temperature was 70˚C, as

specified. The Globe Technologies Model A link was experimentally determined to have a mean activation temperature of 58.3°C with a standard deviation of ±1.5. This finding is higher than the temperature specified by the manufacturer. The Globe Technologies Model K link was experimentally determined to have a mean activation temperature of 57.3°C with a standard deviation of ±0.6.

These results are based on a limited number of experimental tests. For the purposes of this report it is important to be aware that the activation temperature of the links may often exceed the temperature indicated by the manufacturer.

4.4 Conductance Parameter Testing

The procedure discussed in Section 3.2.4, and outlined in Section 2.3.2 was used to determine a parameter value for the conductance. The results for each specific link are shown in Section 4.2.1, Section 4.2.2 and Section 4.2.3. The value obtained for the RTI was as expected per the definition of RTI (NFPA 13, 2007), which states that RTI values be greater than 80 (meter-seconds)$^{1/2}$. Other literature suggests that standard RTI values for fusible link sprinklers significantly higher than the 80 (meter-seconds)$^{1/2}$ (Isman, 2006). As a general guide, because the values of RTI and C' are intertwined a comparison to expected RTI values was done to verify the use of the determined conductance parameter.

4.4.1 Riley Air Link

Using the inputs provided by experimental data from a plunge test and a ramp test in which Riley Air Links were used, the solution to the system of equations yielded the two unknown parameters. These two parameters are conductance (C') and Response Time Index (RTI). The testing showed that the RTI was equal to 138 (meter-seconds)$^{1/2}$ and the conductance parameter, which is the input for C' in Equation (17), is equivalent to 0.02.

4.4.2 Globe Technologies Model A Link

Using the inputs provided by experimental data from a plunge test and a ramp test in which Globe Technology Model A Links were used, the solution to the system of equations yielded the two unknown parameter, conductance (C') and the Response Time Index (RTI). The testing showed that the RTI was equal to 177 (meter-seconds)$^{1/2}$ and the conductance parameter, which is the input for C' in Equation (17), is equivalent to 0.003.

4.4.3 Globe Technologies Model K Link

Using the inputs provided by experimental data from a plunge test and a ramp test in which Globe Technology Model K Links were used, the solution to the system of equations yielded the two unknown parameter, conductance (C') and the Response Time Index (RTI). The testing showed that the RTI was equal to 145 (meter-seconds)$^{1/2}$ and the conductance parameter, which is the input for C' in Equation (17), is equivalent to 0.004.

4.5 Thermal Creep Test

Each of the three links was tested for thermal creep using the procedure described in Section 3.1. Over the period of three days it was observed that there was no significant thermal creep in any of the fusible links.

It is important to consider that this experiment was performed over a short period of time and in order to accurately test for the thermal creep tests with greater longevity and varying conditions would be required.

4.6 Calculated Results Model Verification

In order to compare the model's predictions with the experimental results specific data from the experiments is required to be entered by the user. These inputs include the following;

- Ambient Air Temperature (˚C)

- Wind speed passing over the links (m/s)[1]
- Link Geometry (including length, width, thickness) (m)[2]
- Link emissivity
- Mass of the link (kg)
- Specific Heat of link (J/kg ˚C)

After inputing these experimental values into the thermal response model the results of the model are compared with the experimentally determined results.

4.6.1 Riley Air Link (70°C Activation)

Fast Profile:

When exposed to the fast profile, discussed in Section 2.1, with full frontal exposure to the radiant panel the 70°C Riley Air links were observed to activate at 73 (25_01_07-T2 (Left)) and 71 25_01_07-T2 (Right) seconds. Table 4-9 compares the observed activation times with the model's predicted activation time. Each link experimentally failed within one second of the thermal response model's predicted times.

Fast Profile Data					
Test	Link Description	Activation Time	Predicted Time	Difference	Notes
25_01_07-T2 (Left)	70C Link, VF=1, With Radiometer Paint (ε= ~.9)	73 seconds	673 seconds	1 seconds	N/A
25_01_07-T2 (Right)	70C Link, VF=1, With Black Radiometer Paint (ε= ~.9)	71 seconds	73 seconds	2 seconds	N/A

Table 4-9: Riley Air Link Activation Time Comparison

Figure 4-10 and Figure 4-11 qualitatively represent the accuracy of the model by comparing the thermal response model calculations with the experimental data of two different Riley Air Links.

---

[1] In this report all wind speeds were recorded. In the process of verifying the use of the model to specific experimental results these experimentally measured wind speeds serve as the inputs into the thermal response model. The recorded wind speeds varied from approximately 4 m/s to 10 m/s and are listed in the Appendix of this report.

[2] In cases where the link geometry cannot be assumed to be rectangular, the user of the model is required to determine the volume of the link as well as the area. The inputs for length, width and height should be ignored and the input into the value for the characteristic length should be the ratio of the volume to the area of the link, essentially this value should be close to the thickness of the plate. This is discussed in the calculation of the Reynold's number.
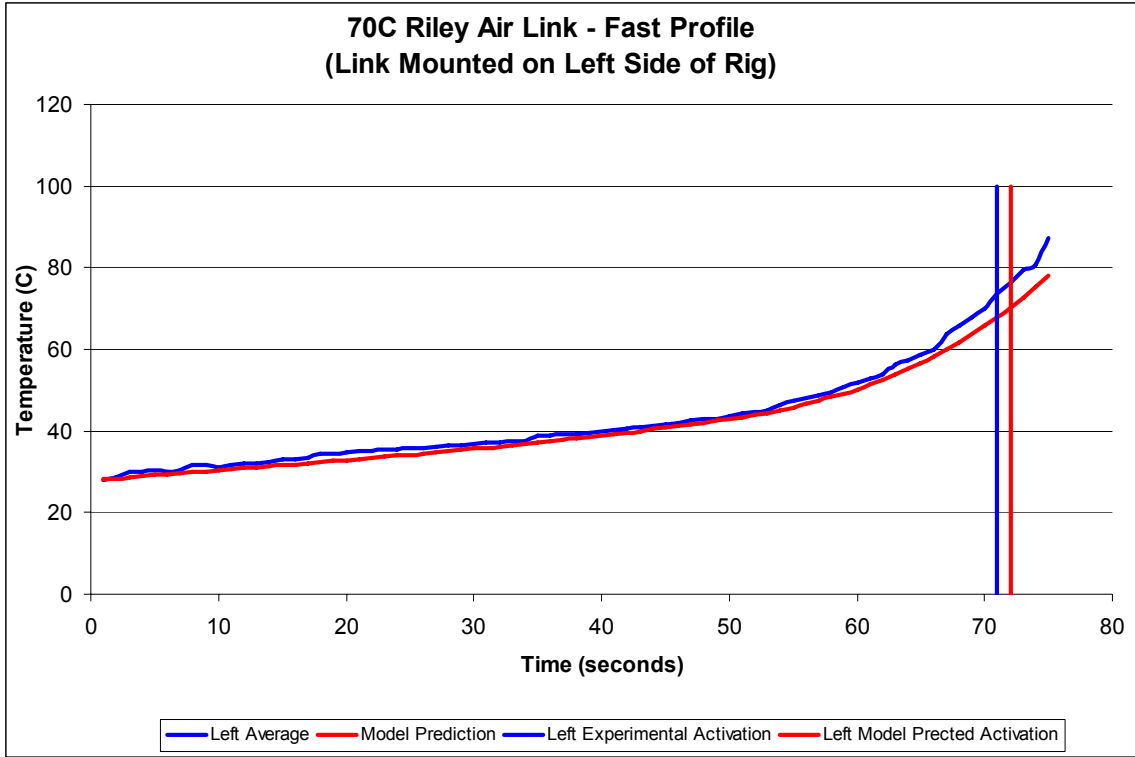
Figure 4-10: Riley Air Link - Painted Black - Exposed to Fast Profile (mounted on left) (25_01_07-T2 (Left))
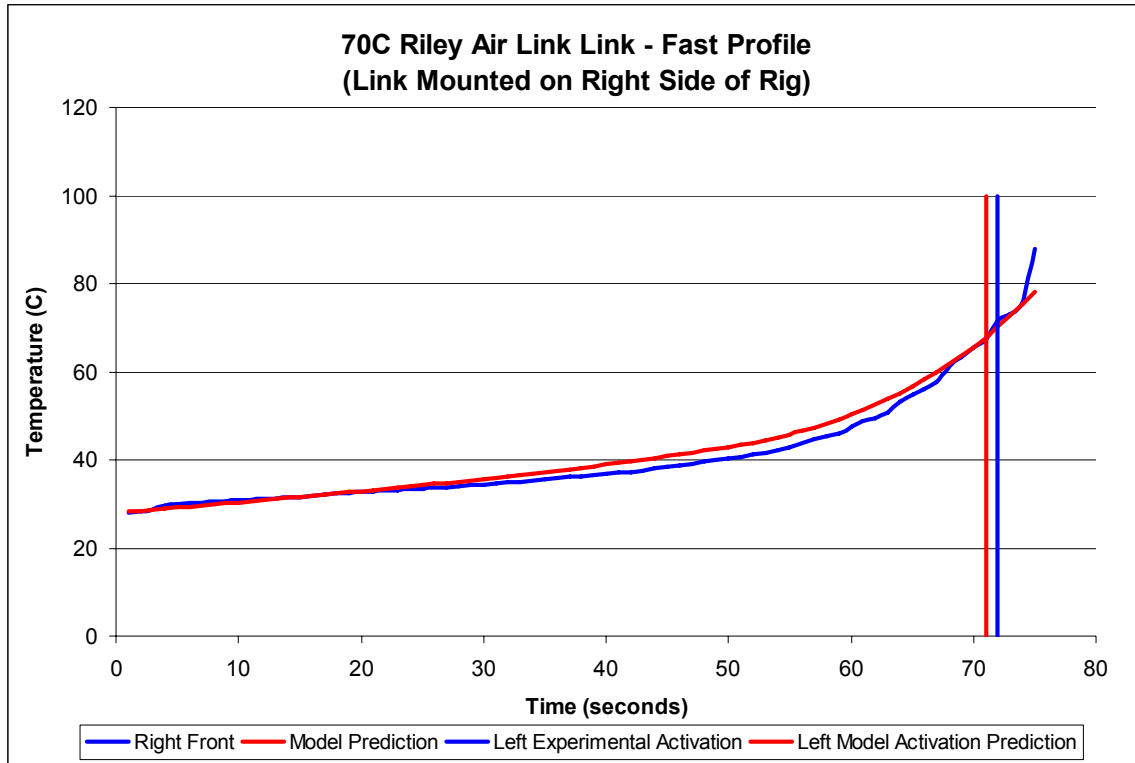
Figure 4-11: Riley Air Link - Painted Black - Exposed to Fast Profile (mounted on right) (25_01_07-T2 (Left))

In each test, two fusible links were tested. On each link a thermocouple was mounted on the front and back face measuring surface temperature, as explained in Section 3.1.1. For each thermocouple the relation to the model's predictions were calculated using the R^2 value, as explained in Section 3.2.6. The results from these calculations indicate that the R^2 values were 0.819 (25_01_07-T2 (Left)) and 0.823 (25_01_07-T2 (Right)) for the model's prediction of the experimental data for the left and right links (respectively).

Slow Profile:

When exposed to the slow profile, the 70°C Riley Air Link activated between 460 (25_01_07-test 1(a)) and 475 (25_01_07-test 1(b)) seconds. This was slightly faster than the calculations of the thermal response model predicted times, but by less than 3% of the total response time. The experimental activation times and the model's predicted activation times are shown in Table 4-10.

Riley Air Link Fast Profile Data					
Test Number	Link Description	Experimental Activation Time	Model's Predicted Activation Time	Difference	Notes
25_01_07-test1 (a)	70C Link, VF=1 with Black Radiometer Paint	475 seconds	480 seconds	5 seconds	N/A
25_01_07-test1 (b)	70C Link, VF=1 with Black Radiometer Paint (Left)	460 seconds	476 seconds	16 seconds	N/A

Table 4-10: Experimental vs. Predicted Activation Times

Plotting the time temperature profiles of the experimental data and the model's predictions qualitatively shows that there is similarity between the calculated and experimental results; this can be seen in Figure 4-12 and Figure 4-13.
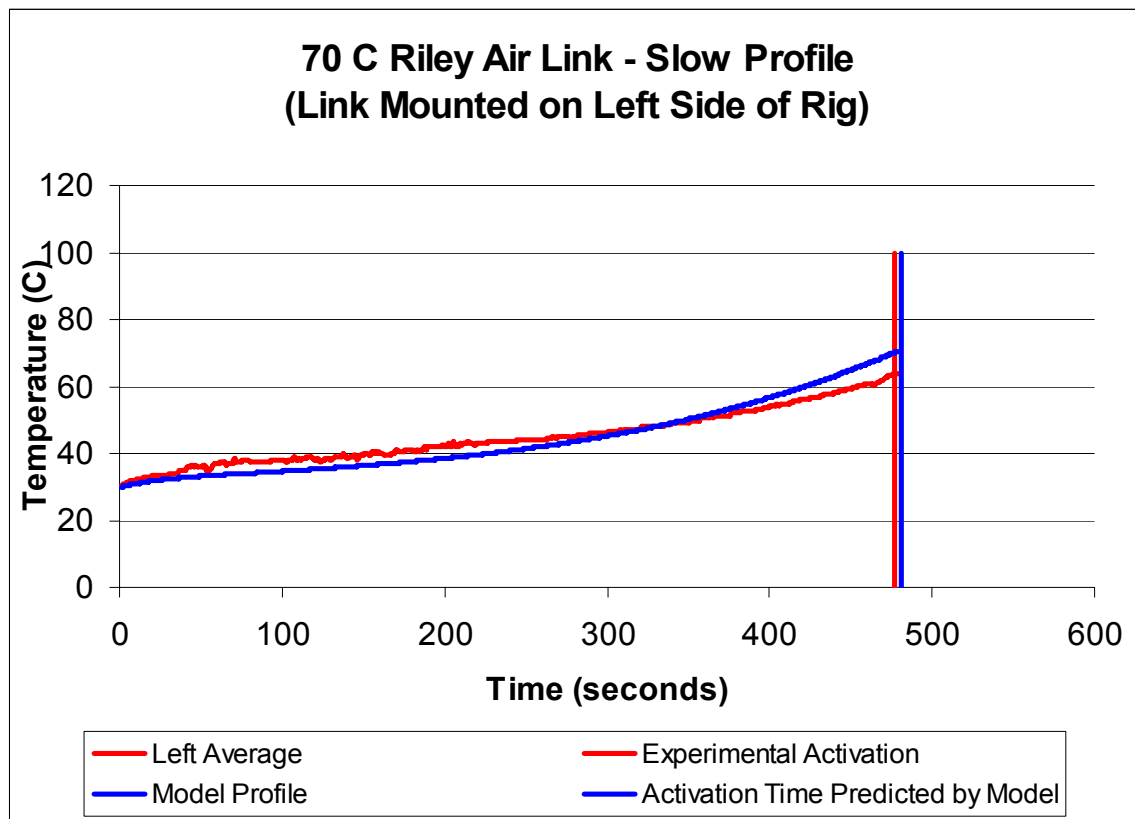
Figure 4-12: Riley Air Link - Painted Black - Exposed to Slow Profile (mounted on left side of test rig)(25_01_07-test 1(a))
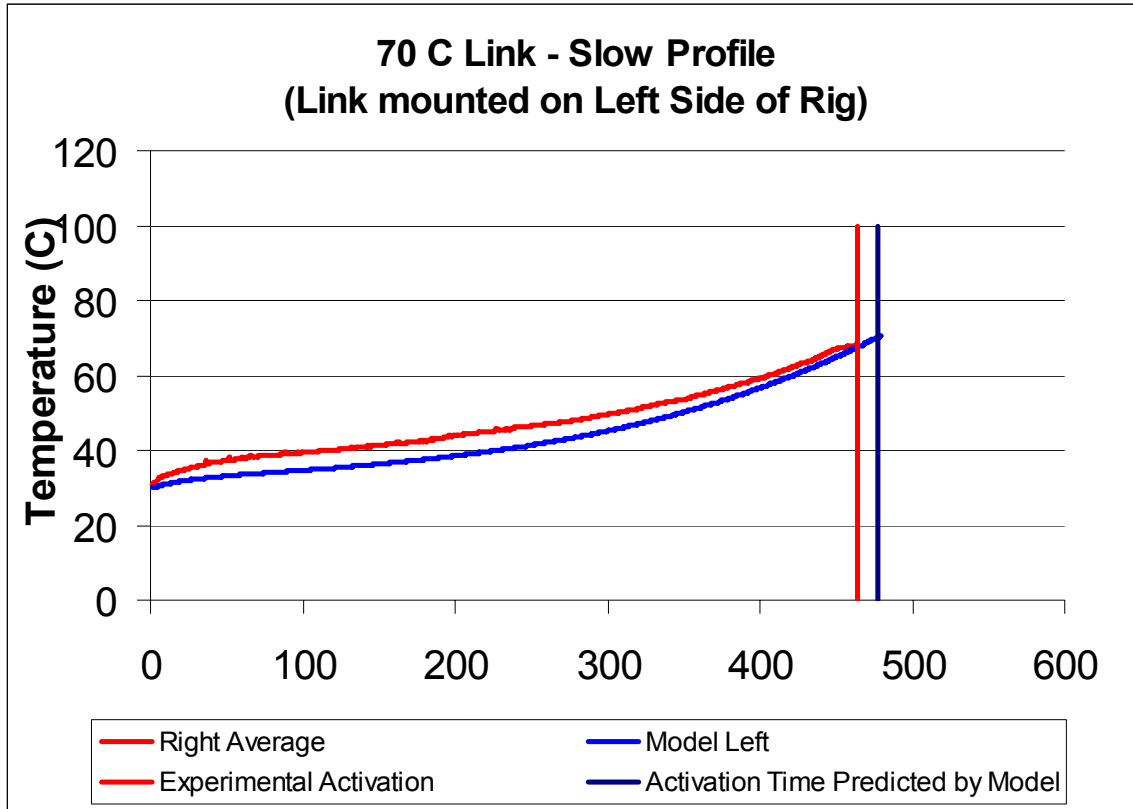
Figure 4-13: Riley Air Link - Painted Black - Exposed to Slow Profile (mounted on right side of test rig) (25_01_07-test1(b))

A statistical analysis using the R^2 method, described in Section 3.2.6 was used to determine the strength of the thermal response model compared to simulated experimental conditions. These calculated values of R^2 for the Riley Air Link exposed to the slow radiation profile resulted in an R^2 values of 0.814 (25_01_07-test1(a)) and 0.862 (25_01_07-test1(b)) for the links mounted on the left and right side of the test rig.

As discussed in Section 4.2, the change of phase parameter for the Riley Air Link was not determined by experimental testing, as done in the case Globe Technology links, however a value of 0.8 was assumed based on the experimental data from the Globe Technologies Link, which had a similar geometry and solder configuration.

4.6.2 Globe Technologies Model A Link (57∘C Activation)

Fast Profile:

A Globe Technologies 57°C, which was found to have an activation temperature greater than the specified 57°C. The link, with emissivity (ε= ~0.9) was experimentally exposed to the fast radiation profile, these results were then compared to the thermal response model's predictions. The experimental activation times are compared with the model's predicted activation times as displayed in Table 4-11. These results are one measure indicating the model's predictive power.

57°C Globe Model A Link Fast Profile					
Test Number	Link Description	Activation Time	Predicted Time	Difference	Notes
31_01_07-T2(a)	57C Model A Link, VF=1, With Radiometer Paint (ε=~0.9) (Left)	69 seconds	68 seconds	1 second	N/A
31_01_07-T2(b)	57C Model A Link, VF=1, With Black Radiometer Paint (ε=~0.9)	67 seconds	68 seconds	1 second	N/A

Table 4-11: Globe Technologies Model A Link Fast Profile Predicted vs. Experimental Activation Times

Figure 4-14 and Figure 4-15 represent plots of the experimental data with the thermal response model to create a time-temperature curve. This qualitative assessment is one indicator of the models strength. A statistical analysis was done using the R^2 method, described in Section 3.2.6.
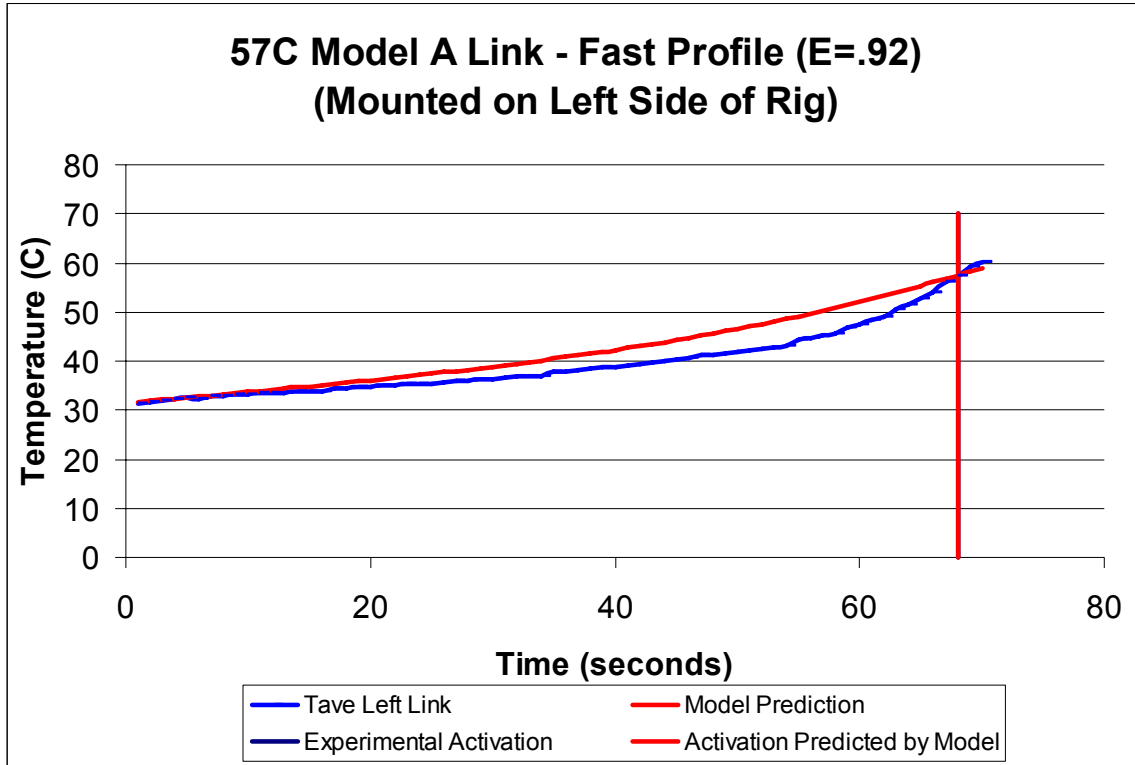
Figure 4-14: Globe Technologies Model A Link Time Temperature Plot (Fast Profile) (mounted on left) (31_01_07-T2(a))
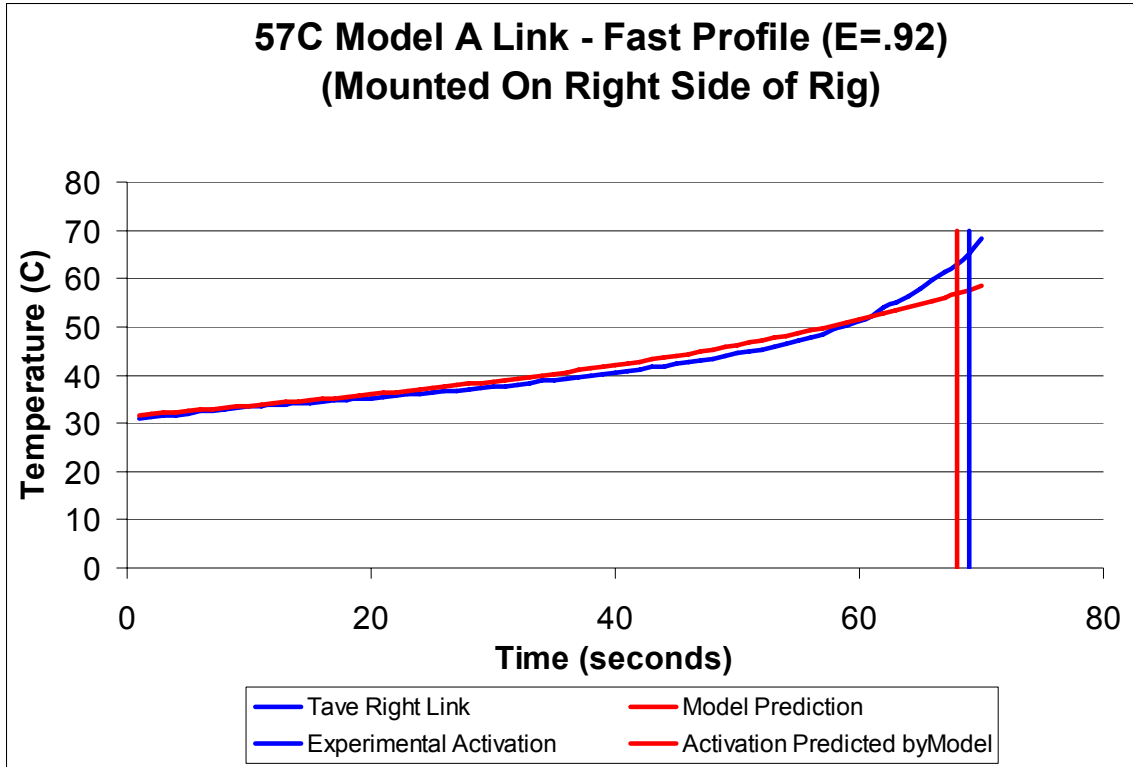
Figure 4-15: Globe Technologies Model A Link Time Temperature Plot (Fast Profile) (mounted on right) (31_01_07-T2(b))

A quantitative analysis using the R^2 analysis indicated values of 0.84 (31_01_07-T2(a)) and 0.81 (31_01_07-T2(b)) in comparing the empirical data with the calculated results of the thermal response model. As discussed in the preceding paragraphs the difference between the models predicted activation time and the experimental activation time was less than 5% of the total response time in all tests.

Slow Profile:

The Globe Technologies Links were exposed to the slow radiation profile used in the Bushfire CRC report. The experimental test results were quantitatively compared to the results calculated by the thermal response model. Prediction of activation times can be seen in Table 4-12. From these results the experimental activation time is slightly greater than the predicted activation time.

Fast Profile Data				
Test Number	Link Description	Activation Time	Predicted Time	Difference
31_01_07-T1(a)	57C Model A Link, VF=1 with Black Radiometer Paint	382 seconds	374 seconds	8 seconds
31_01_07-T1(b)	57C Link Model A, VF=1 with Black Radiometer Paint	403 seconds	374 seconds	29 seconds

Table 4-12: Activation Time Comparison (Model vs. Experimental) Globe Technologies Model A Link (Slow Profile)

The experimental results were plotted versus the calculated results of the thermal response model these time-temperature curves can be seen in Figure 4-16 and Figure 4-17. A qualitative assessment of these graphs indicates the relative strength of the model and consistency of the experimental data.
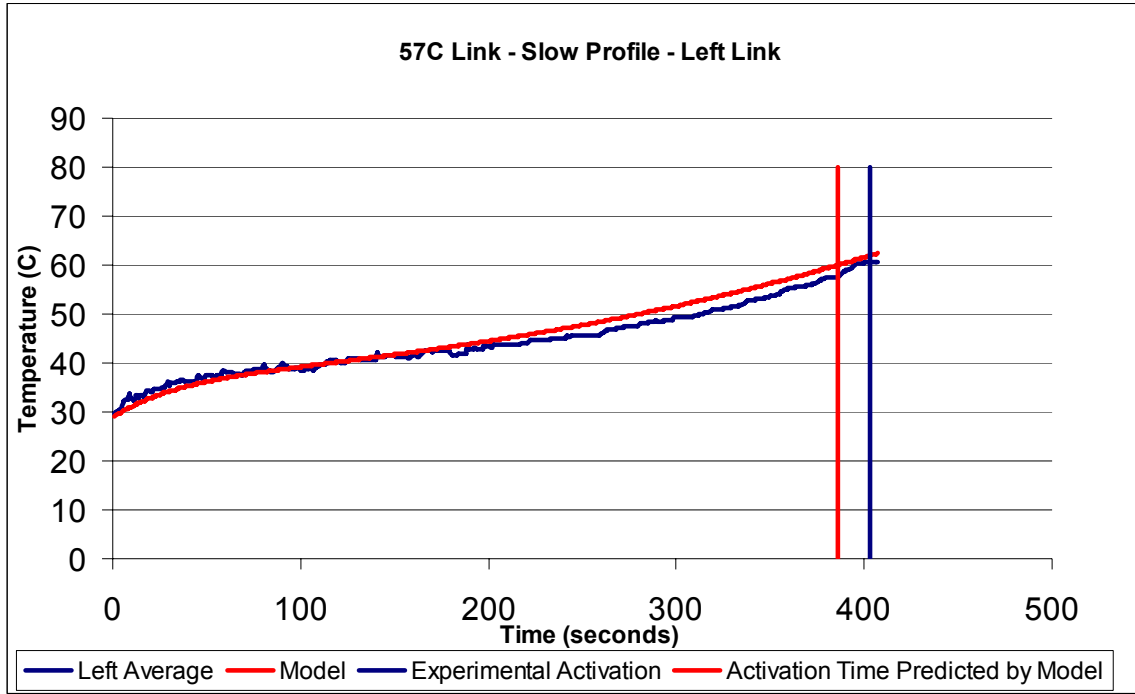
Figure 4-16 Globe Technologies Model A Link Time Temperature Plot (Slow Profile) (mounted on left) (31_01_07-T1(b))
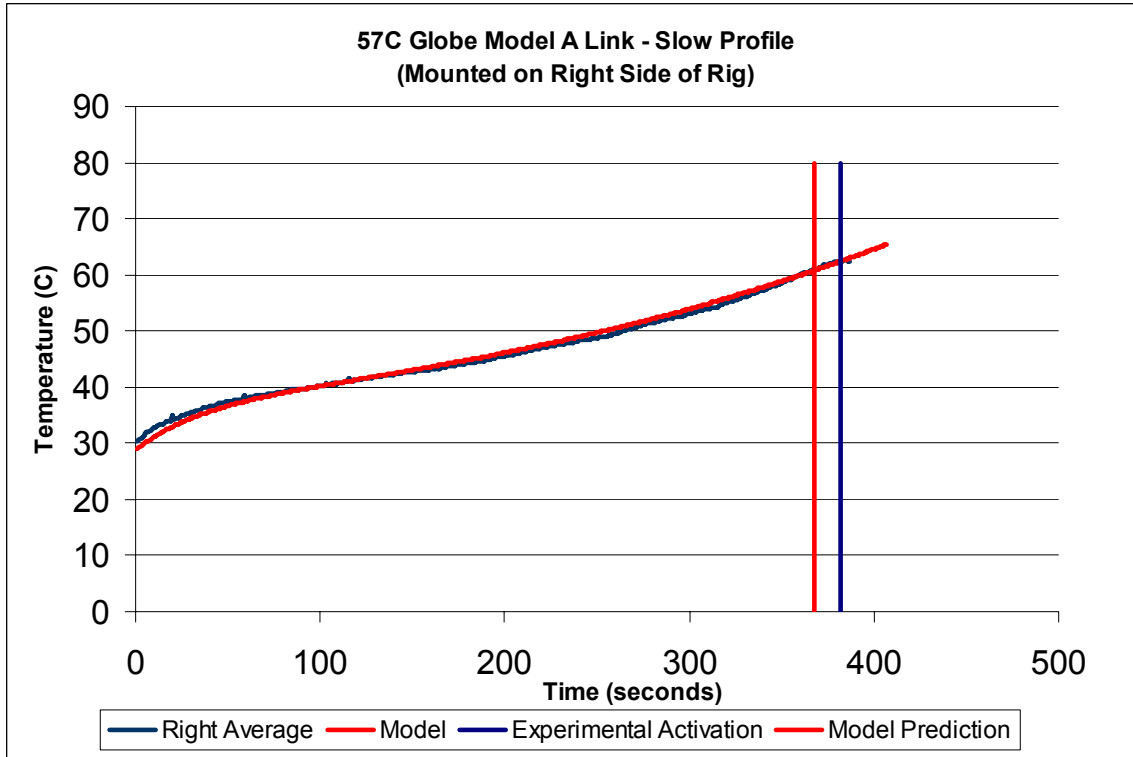
Figure 4-17: Globe Technologies Model A Link Time Temperature Plot (Slow Profile) (mounted on right) (31_01_07-T1(a))

A statistical analysis of the experimental data versus the models predictions was done using the R^2 method. The R^2 values comparing the empirical data with the model's calculations were found to be 0.81(31_01_07-T1(b)) and 0.90 (31_01_07-T1(a)) for the left and right links (respectively) .

4.6.3 Globe Technologies Model K Link (57°C Activation)

Fast Profile:

The Globe Technologies Model K link was tested in the fast profile and the experimental results were used to verify the calculated results of the model. Table 4-13 compares the experimental activation time with the predicted activation time of the thermal response model.

57°C Globe Model K Link Fast Profile					
Test Number	**Link Description**	**Activation Time**	**Predicted Time**	**Difference**	**Notes**
12_02_07test1(a)	57C Model K Link, VF=1, With Radiometer Paint (ε= ~.9) (Left)	67 seconds	63 seconds	4 seconds	N/A
12_02_07test1(b)	57C Model K Link, VF=1, With Black Radiometer Paint (ε= ~.9) (Right)	64 seconds	61 seconds	3 seconds	N/A

Table 4-13: Globe Technologies Model K Link - Fast Profile Predicted vs. Experimental Activation Times

A qualitative comparison of the plots of the experimental and calculated time-temperature profiles is seen in Figure 4-18 and Figure 4-19. This qualitative assessment verifies that the thermal response model is consistently predicting higher temperatures than the experimental data.
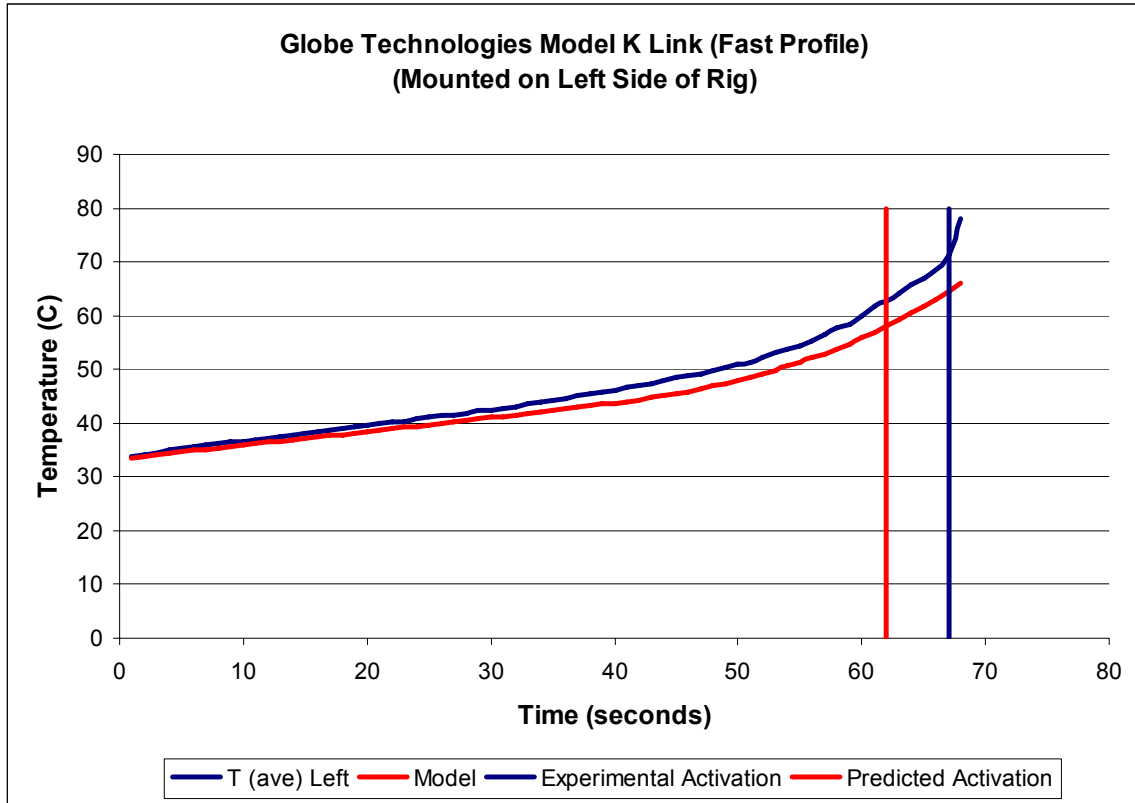
Figure 4-18: Globe Technologies Model K Link Time-Temperature Profile (Fast Profile) (mounted on left) 12_02_07test1(a)
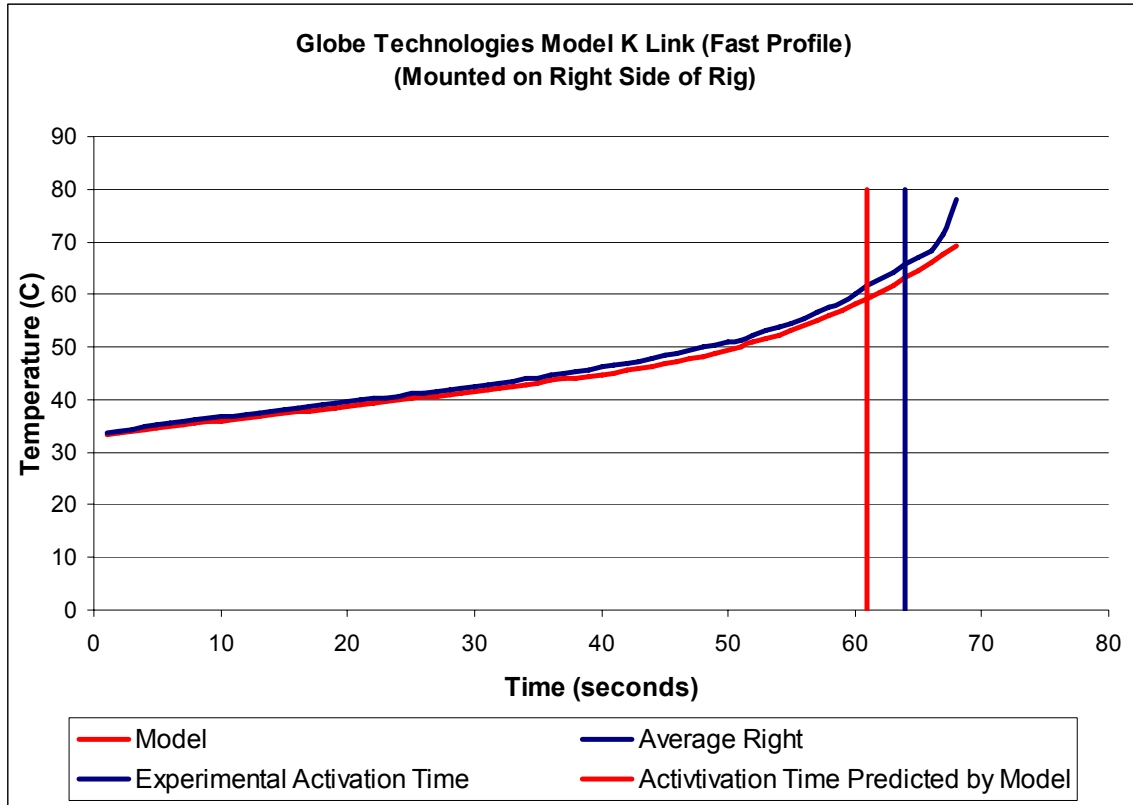
Figure 4-19: Globe Technologies Model K Link Time-Temperature Profile (Fast Profile) (mounted on right) 12_02_07test1(b)

The statistical calculations of the R^2 value based on the results of Figure 4-19 and Figure 4-20 were $R^2=0.81$ (12_02_07test1(a)) and $R^2=0.86$ (12_02_07test1(b)) for links mounted on the left and right (respectively). This statistical evaluation along with the qualitative assessment and predicted activation time and estimated activation time validate the use of the constructed thermal response model.

4.7 Sensitivity Analysis of Validated Model

After verifying the strength of the constructed thermal response models, as done in Section 4.6 the model was used to generate results indicating the individual effects of the heat transfer components and parameters; convection, conduction, emissivity and heat of fusion. Section 4.7.1 shows the sensitivity of these factors based on the calculated results for the Globe Technologies Model A link exposed to the fast. The behavior between the models in both radiation profiles were similar, therefore only one set of data is presented in this report.

In conducting the sensitivity analysis, each parameter is investigated by being increased by 20% and then decreased by 20%. The effect of the change is compared with the behavior of the link exposed to the normal parameter value graphically. These results were also evaluated using the R^2 analysis.

4.7.1 Sensitivity Analysis Globe Model A – Fast Profile (Right Link) Conductance Sensitivity

The sensitivity of the conductance parameter, Section 4.4.2, was analyzed by first increasing and then decreasing the conductance parameter (C') by 20%. The results of this analysis is compared to the plot of the calculated results using the normal conductance parameter, can be seen in Figure 4-20 and Figure 4-21. R^2 values were determined to be 0.999 for both increased vs. normal data and the decreased for normal data. From this finding, it was concluded that conduction losses do not play significant role in the overall heat transfer process in the proposed application.
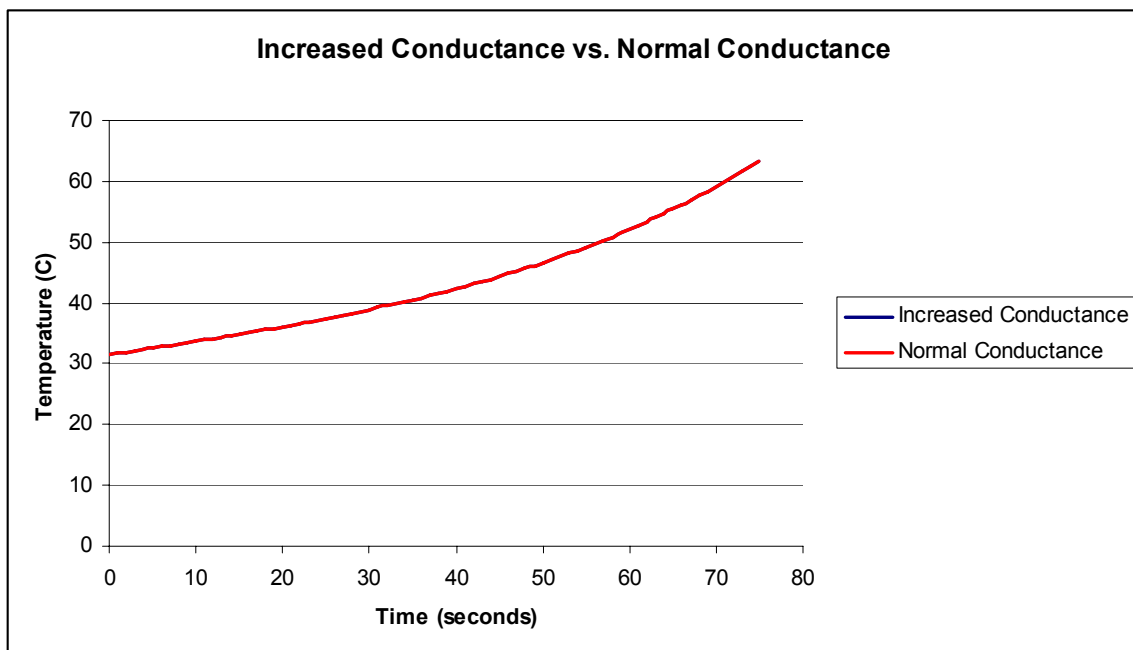
Figure 4-20 Sensitivity Analysis (Fast Profile) Increased Conductance
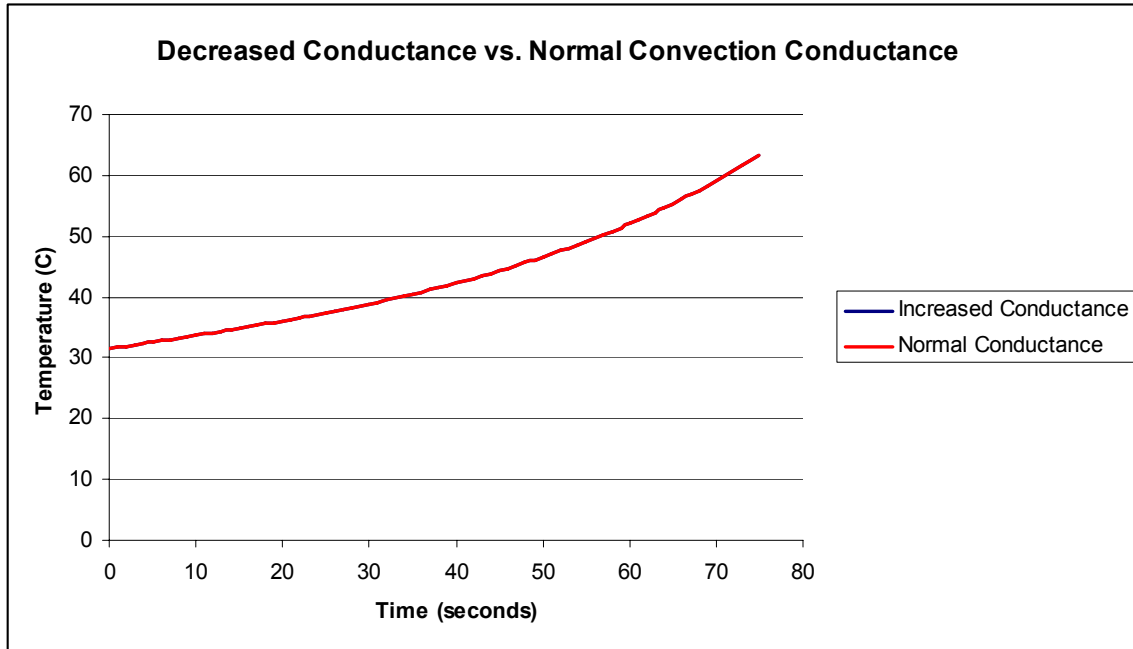
Figure 4-21 Sensitivity Analysis (Fast Profile) Decreased Conductance

Convection Coefficient Sensitivity

The sensitivity of the convection coefficient (h) is dependent on the experimental cooling air speed as well as the assumed geometry of the fusible link. An analysis on this parameter was done to determine the parameter's sensitivity. The results of this analysis compared to the plot of the calculated results using the normal convection coefficient (h) parameter can be seen in Figure 4-22 and Figure 4-23. R^2 values were determined to be 0.995 for the increased vs. normal data and 0.994 for the decreased for normal data. From this it is apparent that the convection coefficient does not play a dominant role in the overall heat transfer process in this application, however is more prevalent than the effect of changes in conductance.
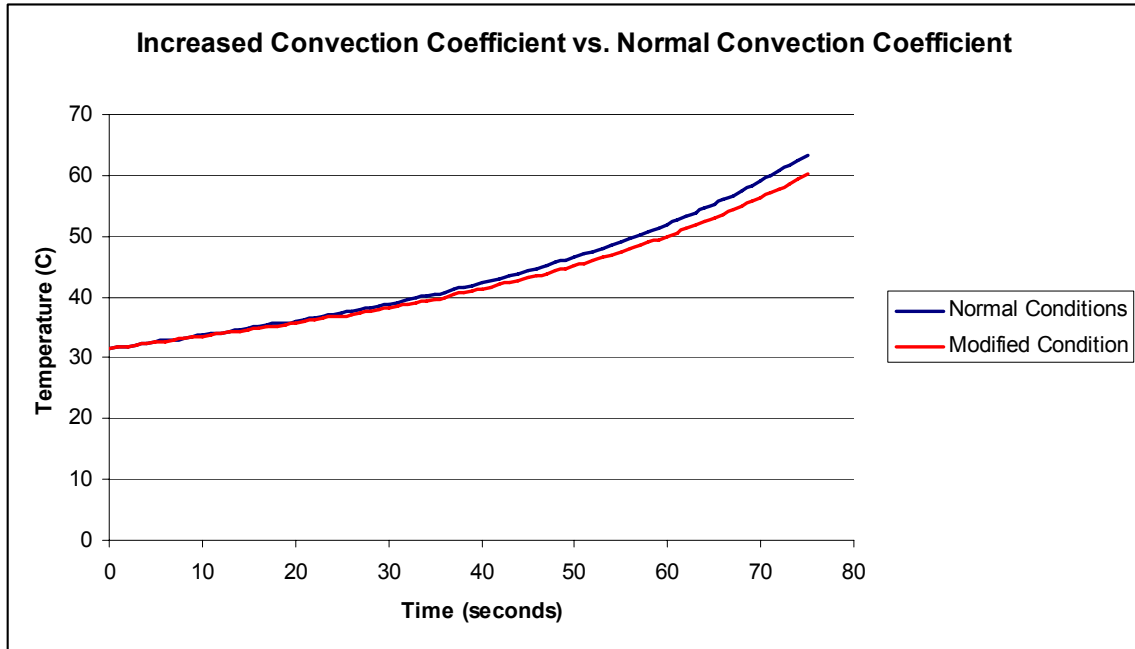
Figure 4-22 Sensitivity Analysis (Fast Profile) Increased Convection Coefficient (h)
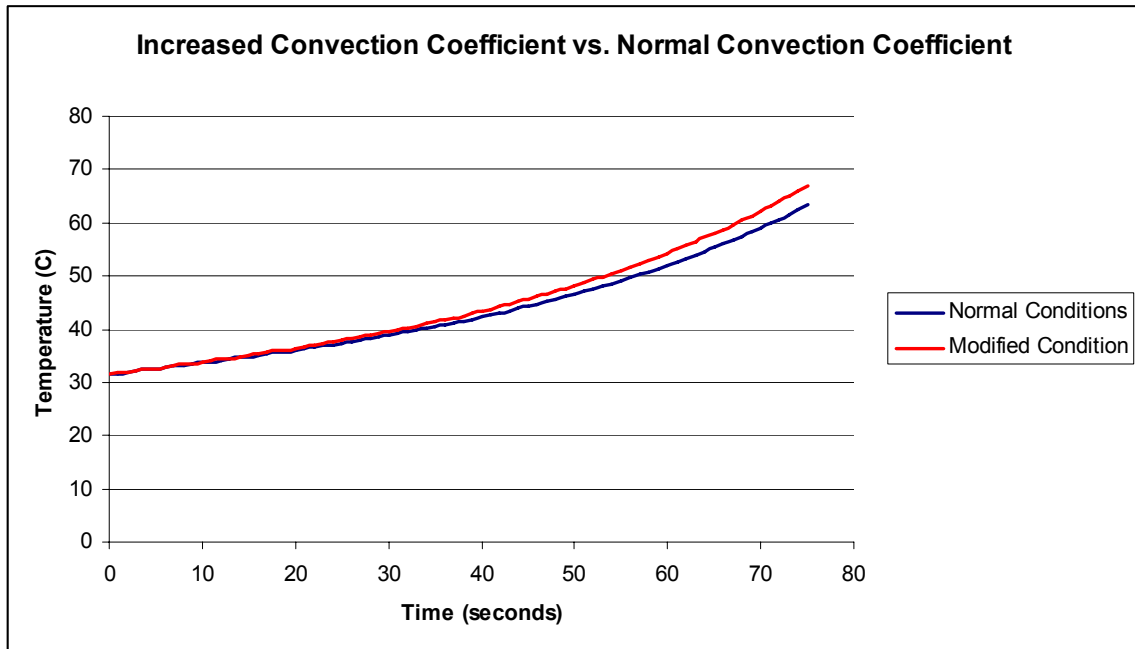
Figure 4-23 Sensitivity Analysis (Fast Profile) Decreased Convection Coefficient (h)

Velocity of Cooling Air Sensitivity

As indicated in the convection coefficient sensitivity, air velocity is a variable in the experimental testing and would be in actual fire scenarios. The isolated effect of this parameter was analyzed and determined to be largely insignificant as shown in Figure

4-24 and Figure 4-25. These figures plot the difference between two velocities with 20% difference. A statistical evaluation supported this finding as R^2 values for each the increased and decreased velocity were $R^2=0.975$ and $R^2=0.971$
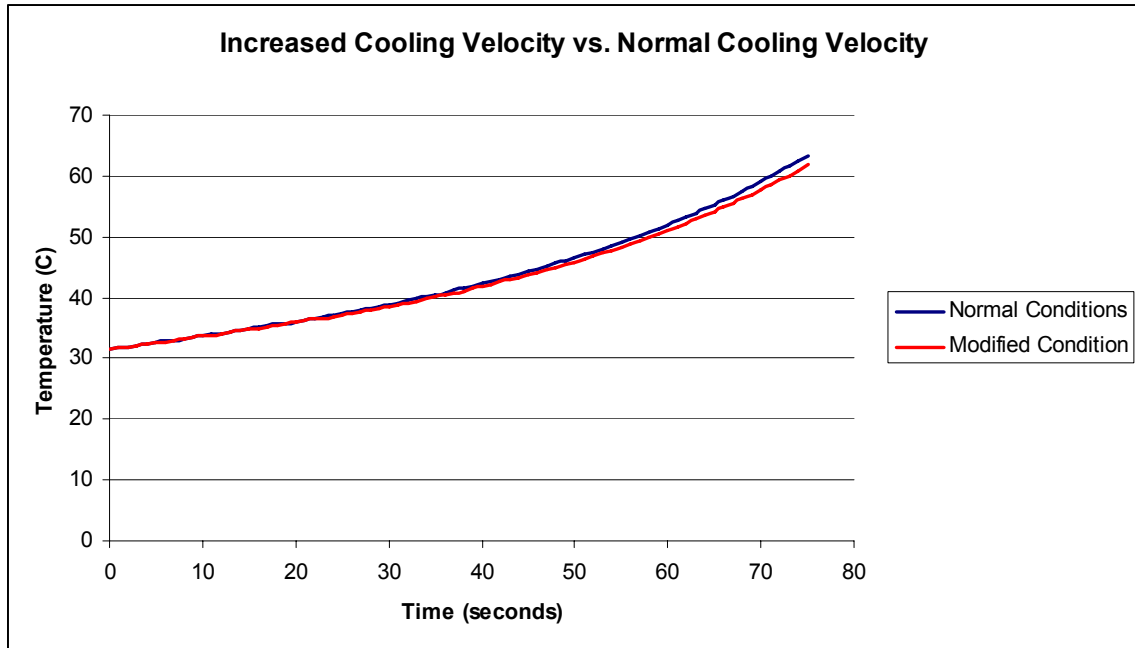
Figure 4-24 Sensitivity Analysis (Fast Profile) Increased Air Velocity
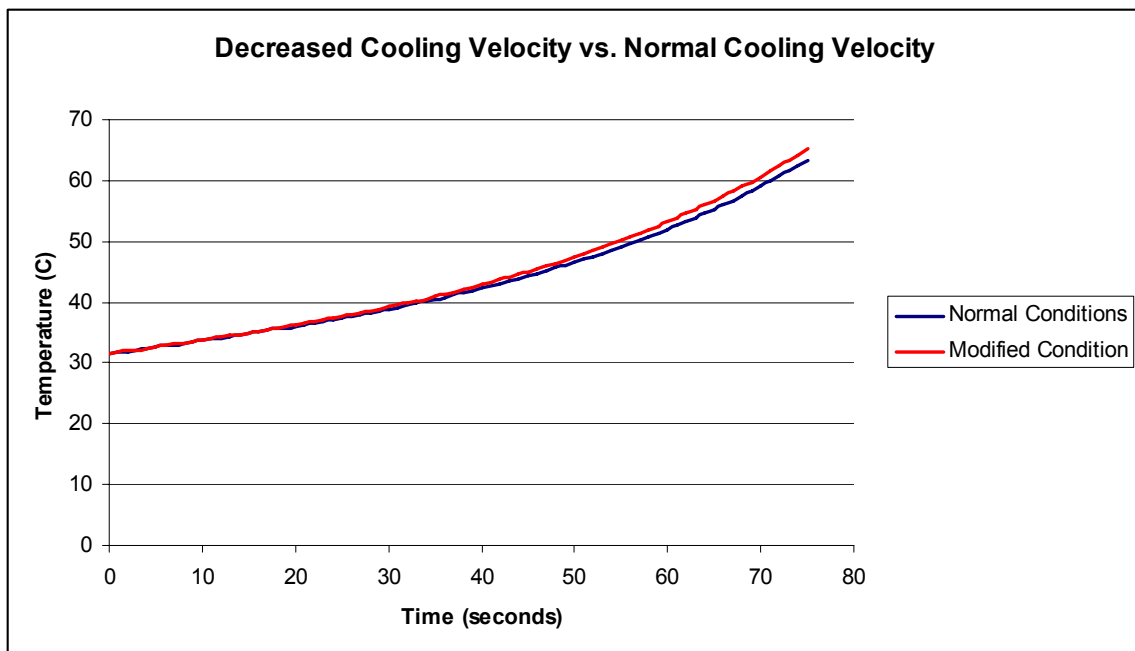
Figure 4-25 Sensitivity Analysis (Fast Profile) Decreased Air Velocity

73

Emissivity Sensitivity

The sensitivity of the link's emissivity was analyzed by first increasing and then decreasing the value of the emissivity by 20%. The results of this alteration compared to the plot of the calculated results using the normal emissivity values can be seen in Figure 4-26 and Figure 4-27. R^2 values were determined to be 0.89 for the increased vs. normal data and 0.889 for the decreased vs. normal data. From this it is apparent that emissivity is a significant heat transfer component, greater than conductance, convection coefficient and cooling air velocity variations.
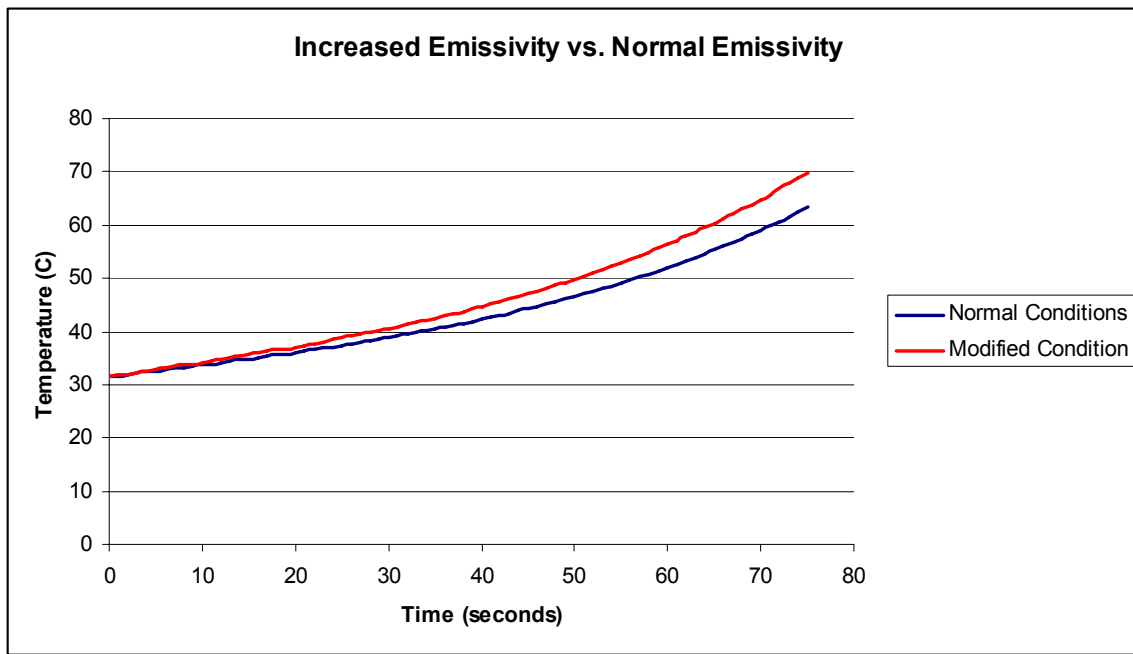
Figure 4-26 Sensitivity Analysis (Fast Profile) Increased Emissivity
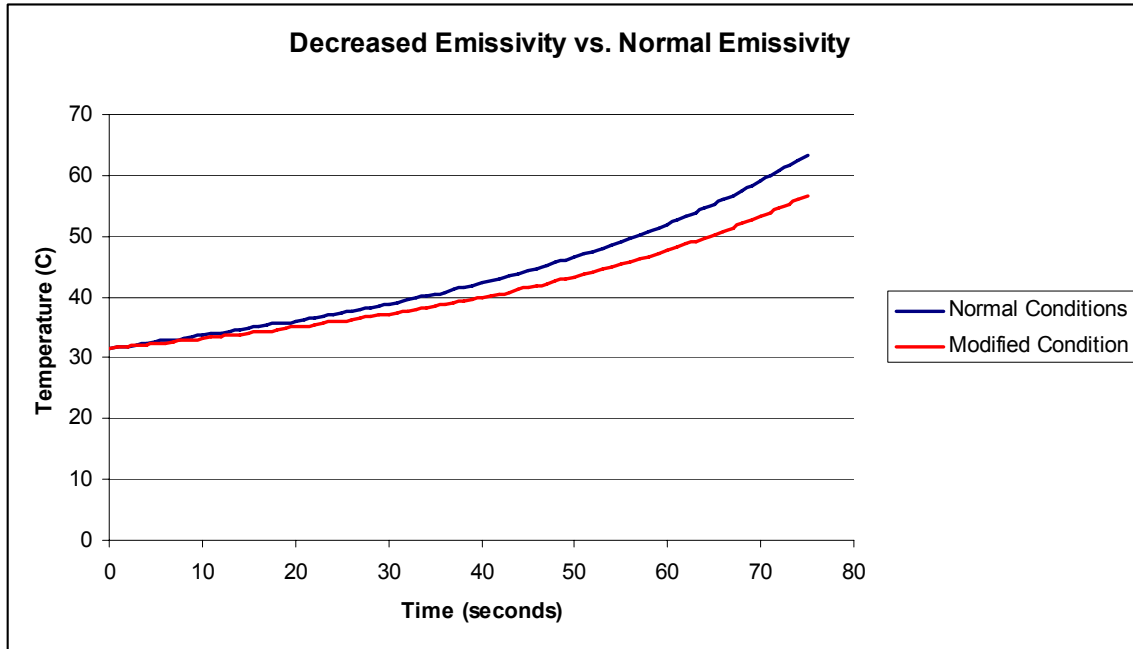
Figure 4-27 Sensitivity Analysis (Fast Profile) Decreased Emissivity

Heat of Fusion Sensitivity

The sensitivity of the link's heat of fusion was analyzed by first increasing the value of the normal CHP parameter by 20% and then decreasing the value of the CHP parameter by 16%, which was all that was permitted before assuming no heat of fusion energy. The results of this alteration compared to the plot of the calculated results using the normal CHP values can be seen in Figure 4-28 and Figure 4-29. R^2 values were determined to be 0.885 for the increased vs. normal data and 0.911 for the decreased vs. normal data. From this it is apparent that change of phase parameter (CHP) is a significant heat transfer component, greater than conductance, convection coefficient and cooling air velocity variations while similar to the effect of emissivity.
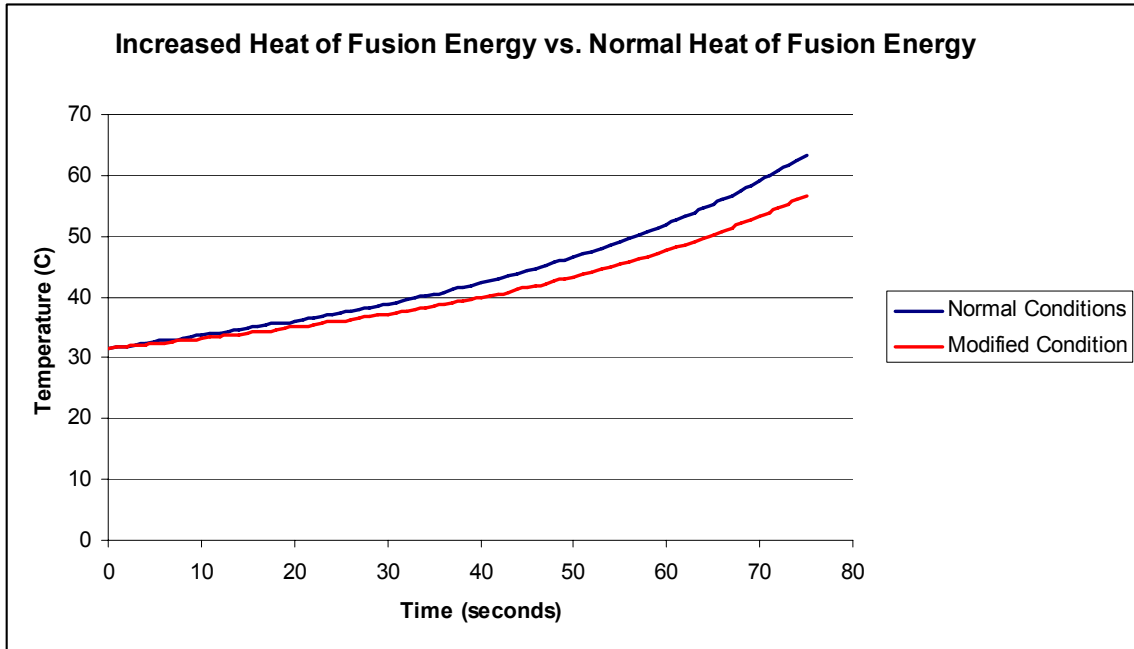
Figure 4-28 Sensitivity Analysis (Fast Profile) Increased CHP
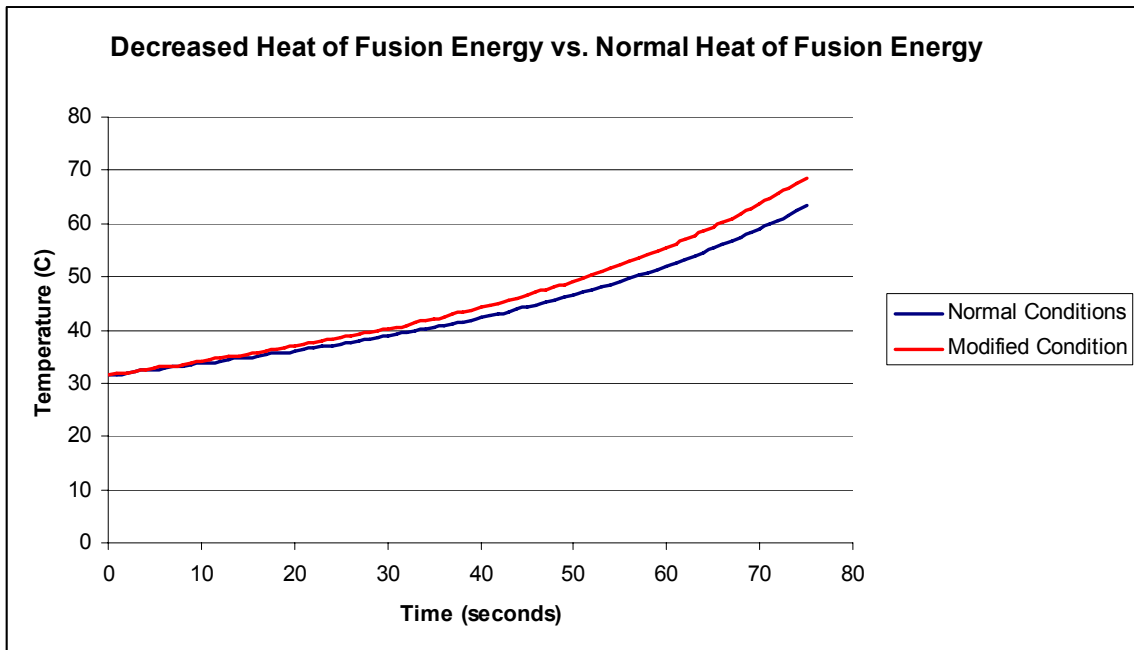
Figure 4-29 Sensitivity Analysis (Fast Profile) Decreased CHP

4.8 Additional Findings

In the early stages of experimental testing there was an attempt to mount the fusible links on the test rig in a way to minimize the potential conduction losses from the fusible link to wire and associated accessories. The method used to minimize the conduction losses was to mount the links with black plastic wire-ties. The fusible links attached by these plastic wire-ties were tested in the fast profile.

In each test it was observed that the plastic wire tie failed prior to the activation of the fusible link, regardless of configuration or emissivity. It was found based on five tests that the average activation time of the plastic wire ties was 76.2 seconds with a standard deviation of ±9.3 seconds, based on 6 tests. As found in Section 4.1.2, the activation time of the unaltered links is greater than the experimentally determined activation time of the plastic wire tires. The unaltered Riley Air Link activated at a mean 92.5 seconds with a standard deviation of ±35.5 seconds. The unaltered Globe Technologies Model A activated at a mean of 112 seconds with a standard deviation of ±11.14 seconds. The activation times of the links with altered emissivity (ε =~0.9) were slightly lower than the determined activation times of the plastic wire ties.

From this accidental observation it is clear that the use of fusible links is potentially a feasible solution. It was experimentally observed that the plastic ties failed prior to the 85 seconds performance required specified by the performance based design aspect of this project.

Creep testing was also done on the plastic wire ties, as done was each of the fusible links. The results from this showed that over a three day period exposed to constant 50°C oven temperatures and an applied load of 10 kg the plastic wire-ties experience negligible thermal creep.

There are a number of concerns with using plastic wire ties in this outdoor application such as long term thermal creep and the homeowner using unspecified plastic wire-ties which may not necessarily activate prior to the failure of a window. Additional work is

suggested in exposing plastic wire ties to different radiation profiles and long term

exposure to actual environmental conditions within Australia.

5 Conclusions

5.1 Performance Based Design Conclusions

The goal of this project was to find a method of automatically closing a fire door or shutter assembly which protects a window when exposed to wildfire conditions. A number of potential solutions were developed in the design process. The most feasible solution from the design process was that fusible links were the most viable solution. In this application fusible links would serve as the means of automatic activation of the fire door which would be closed by a simple pulley and counter-weight system. The performance objective of the project was to ensure that fusible links would activate, thereby closing the fire door or shutter protecting a window, prior to window barrier failure when exposed to wildfire conditions.

Window performance and failure times when exposed to wildfire simulated conditions were documented in a report released by the Bushfire CRC in 2004. This report specified that 5 mm toughened glass windows could withstand up to 580 seconds when exposed to a slow radiation profile and would not fail when exposed to a fast radiation profile with peak heat fluxes at 40 kW/m^2. Additional data from the literature review specified that toughened glass windows could withstand up to 40 kW/m^2 before failing. An evaluation of radiation measurements taken from experimentally simulated wildfires of the International Crown Fire Modeling Experiment clearly indicated that wildfires with radiation profiles often exceed 40 kW/m^2. Based on this experimental data from the ICFME the time it took to reach 40 kW/m^2 was determined, 85 seconds. As a results 85 seconds was assumed to performance activation time objective when exposed to a fast radiation profile. Based on the results of the Bushfire CRC report and the International Crown Fire Modeling Experiment the activation time objectives for the fusible links were 580 seconds for a slow radiation profile and 85 seconds for a fast radiation profile.

The performance of fusible links in wildfire conditions was determined experimentally using test apparatus constructed at the CSIRO Bushfire Research Laboratory. Experimental tests showed that the activation time of unaltered links in the fast profile

would exceed the specified performance objective activation times. However, when links were painted with black radiometer paint, the links activated well within the specified performance objective times. Similar results were found for the fast profile, as the links' emissivities were altered the activation times significantly dropped and were below the specified performance objection of 580 seconds. The test were performed at ambient air temperatures between 15˚C and 30˚C and air speeds of approximately 4 (m/s) – 10 (m/s) passing over the links to simulate convective cooling.

In conclusion the performance based objective, when the specified links are painted with black radiometer paint their use as a means of automatic activation for fire doors is satisfied. However, when links are unaltered the performance based objectives are not met and it is not acceptable to use fusible links in the proposed application.

5.2 Heat Transfer Processes

Experimental data was used to verify the use of a computer based model which calculated the temperature of the fusible link (and consequently the activation time) in a transient heat transfer process. This model was required to account for energy storage, incident radiation, convective cooling, conduction losses, heat of fusion energy, and radiation losses of the fusible link.

This model provides inherent value to future performance based design considerations as the user is required to specify the incident radiation profiles. The user is also capable of changing linkages by altering values for surface area, volume, thermal properties (including RTI and the heat of fusion parameter).

The calibrated model was also used to determine the dominant modes of heat transfer and critical parameters influencing the fusible link. From this work it was determined that conduction from the fusible element to the link and associated attachments is negligible while the most significant parameters are the heat of fusion parameter and the value of the emissivity.

6 References

Beckwith, Thomas G and Roy D. Maragoni. <u>Mechanical Measurements</u>. Ed. Marcia J.
Horton. Upper Saddle River, NJ: Peason Prentice Hall, 2007.

Butler, B.W., J. Cohen, D.J Latham, et al. <u>Measures of Radiant Emmissive Power and
Temperatures in Crown Fires</u>. Canada: National Research Council (NRC) -
Canada, 2003.

<u>Climate Statistics for Australian Locations</u>. 2007. Australian Government: Bureau of
Meteorology. n.d.
<http://www.bom.gov.au/climate/averages/tables/cw_086077.shtml>.

Debnam, Glenn. Ed. Vincent Chow and Paul England. Sydney, Australia: Warrington
Fire Research Ply. Ltd., 2005.

Evans, David D and Daniel Madryzkowski. <u>Characterizing the thermal response of
fusible-link sprinklers</u>. Washington D.C.: National Bureau of Standards, 1981.

Factory Mutual Approvals. <u>Approval Standard for Heat Responsive Links For Fire
Protection</u>. Norwood, MA: FM Approvals LLC., 2002.

Fox, Robert W, Alan T. McDonald, and Phillip J. Pritchard. <u>Introduction to Flud
Mechanics</u>. Ed. Jenny Welter. Danvers, MA: John Wiley and Sonss, 2006.

Gustafsson, N.E.A. <u>A Three Parameter Model for Characterizing Sprinkler Sensitivity
and Predicting Sprinkler Activation Times</u>. N.p.: C.E.A Subcommittee, 1988.

Heskestad, G and H.F. Smith. <u>Investigation of a New Sprinkler Sensitivity Approval
Test; The Plunge Test</u>. Norwood, MA: Factory Mutual Research Corporation,
1976.

Heskestad, G. and R.B. Bill. <u>Conduction Heat-Loss Effects on Thermal Response of Automatic Sprinklers</u>. Norwood, MA: Factory Mutual Research Corporation, 1987.

Incorpera, Frank P, David P. DeWitt, Theodore L. Bergman, et al. <u>Fundamentals of Heat and Mass Transfer</u>. Ed. Joseph Hayton. Danvers, MA: John Wiley and Sons, 2007.

Isman, Kenneth E. "Do Quick Response Sprinklers Provide Better Fire Protection." <u>Fire Protection Engineering</u> 1 6 Feb. 2006: N. pag. n.d. <http://www.fpemag.com/archives/enewsletter.asp?i=1>.

Job, E.J., N.J. Job, and J.R Paetow. <u>Remarks on Theory and Testing for Sprinkler Sensitivity</u>. Ahrensburg: n.p., 1990.

Meacham, Brian J. <u>Extreme Event Mitigation in Buildings : Analysis and Design</u>. Ed. Matthew A. Johann. Quincy: Na, 2006.

Mowerer, Frederick W. <u>Window Breakage Induced By Exterior Fires</u>. College Park, Maryland: National Institute of Standards and Technology (NIST), 1998.

National Fire Protection Association (NFPA). <u>NFPA 1144: Standard for Protection of Life and Property from Wildfires</u>. Ed. Steinberg Michelle. Quincy, MA: National Fire Protection Association, 2002.

National Fire Protection Association. <u>NFPA 72: National Fire Alarm Code</u>. Ed. Lee Richardson. Quincy, MA: National Fire Protection Association, 2007.

National Fire Protection Association. <u>NFPA 13: Standard for the Installation, Inspection</u>
<u>and Maintenance of Automatic Sprinklers</u>. Ed. Christian Dubay. Quincy, MA:
National Fire Protection Association, 2007.

Poon Ph.D, Leong. <u>Literature Review of Bushfire Construction Materials and Test</u>
<u>Protocols for Performance Assessment</u>. Ed. J.P. England. Sydney, Australia:
Warrington Fire Research Ply. Ltd., 2002.

Ross, Shepley L. <u>Introduction to Ordinary Differential Equations</u>. Ed. Shepley L. Ross II.
Danvers, MA: John Wiley and Sons, 1989.

Schiffiliti, Robert P, Brian J. Meacham, and Richard L. Custer. "Design of Detection
Systems." <u>SFPE Handbook of Fire Protection Engineering</u>. Ed. Phillip J.
DiNenno. Quincy, MA: National Fire Protection Association (NFPA), 2002. N.
pag.

Swedish National Testing and Research Institute. <u>Thermal Response Models for Glass</u>
<u>Bulb Sprinklers</u>. Ed. Haukur Ingason. Boras, Sweden: Fire Technology, 1994.

Warrington Fire Research Consultancy. <u>Guidelines for Evaluation and Specification of</u>
<u>Bushfire Resistant Building Elements</u>. Sydney, Australia: Warring Fire Research
Consultancy, 2004.ton

Webb, Alex. Online interview. 19 Apr. 2007.

Appendix A: Design Process

1) Identification of Need:

A method of automatically closing a wildfire screen (often regarded as fire doors/shutters) prior to the failure (cracking, internal flaming or shattering) of windows potentially exposed to wildfires.

2) Background Research

Background research is required to be done in the following areas:
- General wildfire hazards to property
- Wildfire fire data (radiant exposures, temperatures, relative speed)
-.Window performance data (failure points, methods)
- Existing methods for application (fusible link data)
- Performance requirements of particular application (loading requirements, ambient conditions, required activation temperature and time)

3) Goal Statement

To design and prove through experimentation a method to automatically activate a wildfire screen prior to window failure.

4) Performance Specifications

The main performance specification in this performance based design is to find a reasonable means of activating a wildfire screen assembly when exposed to a wildfire conditions prior to window failure. Because this is a performance based design there is flexibility in how this performance specification is met. This process of activating a wildfire screen is required to be done in two interconnected steps:

1.) Detection of wildfire conditions
2.) Actuation of wildfire screen (fire door/shutter)

Additional performance criteria are listed as follows:
 - Loading requirements
Because there a number of means of detection the loading requirement will affect each design differently. Not all means of detection are required to be capable of supporting an assembly load (specific to the loads in each application). In cases where detection devices are load bearing they shall be capable of holding and sustaining the applied loads (actual assembly loads) of normally holding the door open (including associated pulleys, counterweights, gravitational forces, tensions provided by motors etc.). In cases where the detection device are not load bearing, additional devices or mean shall be in place to normally hold the door open. In both cases the minimum required load must keep the door unless actuated by a wildfire detection device (or inspection).

 - Operating temperatures

The wildfire screen must operate prior to levels of temperature and radiation exposure from wildfires which cause failure in windows. Operation must be in the ambient conditions of Australia, which includes high temperature exposure.

 - Environmental protection
All outdoor components of the application must be effective for a minimum one year in Australia's environmental conditions and prevent against the various types of corrosion, including by not limited to salt, stress cracking, carbon dioxide/sulfur dioxide, hydrogen sulfide.

 - Sensitivity (temperature)
The operating time of the detector in either design shall not exceed the values (of new and aged/elevated temperature) required by FM's Approval Stand for Heat Responsive Links for Fire Protection (Approval Standard 7440) and shall not exceed an activation requirement of greater than 74 C (as required by FM's Approval Standard for Fire Doors- Approval Standard 4100).

- Mechanical operation
In fusible link designs there shall be a zero percent of mechanical failure (no hang ups).

5) Ideation and Invention

1.   Ideation and Invention
   1.1.   Fusible Links
      1.1.1.   **Conceptual Idea:** This is the traditional means of activating a fire door/screen or shutter. An evaluation would entail potentially changing the temperature ratings of these detectors by altering the mass of the link, the material type, the fusible material type, the shape of the link, the orientation of the link (view factors), the emissivity of the link, load.
   1.2.   Plastics / Polymers
      Analysis: This is a very practical and feasible solution. To ensure that the links operate at ideal temperatures a number of modifications can be made and proven through experimentation. A few concerns that we have is the "thermal load" from solar radiation, the configuration and associated view factors, conductive losses (both inside the link and to the associated system), and convective cooling from ambient air.
      1.2.1.   **Conceptual Idea:** In concept this would work similarly to a traditional fusible link, however the material of the link would be a plastic or a polymer and not as sensitive to corrosion and other environmental factors.
        Analysis: This is also a practical and feasible solution, given the proper polymer is chosen (which will activate at a given temperature and absorb radiative exposure from the bush fire. Additionally there is concern in the mechanical properties of plastic such as creep (especially when exposed to hot Australian ambient conditions).
   1.3.   Heat detectors (rate of rise) interfaced with magnet holding system

1.3.1. **Conceptual Idea:** In concept a rate of rise detector would detect the rapid rate of rise from a bush fire and send a signal to a magnetic door holder (which normally would hold the fire door open) and the door holder would then "de-activate" closing the door (or the detection device could activate an electric motor/reel thereby closing the door)

Analysis: This is a non-traditional approach which would be applicable, however the current cost of installing such a device exceeds the budget of this particular application. This is mainly due to the cost of the heat detector and the installation costs. Electric motors on each door/window would also be too costly, however magnetic door holders could be reasonable and reduce the number of required inspection (or at least simplify them)

1.4. Linear heat detectors (thermal fuse) interfaced with magnet holding system

1.4.1. **Conceptual Idea:** Same concept as heat detectors except with a different detector.

Analysis: This is similar to the previous approach and is financially more feasible. Linear heat detectors could be installed in many different areas, on the face of each door (this would be relatively unobtrusive) or in a perimeter at some distance from the house. Detectors would be interfaced with a magnetic door holder, so when the linear heat detector is activated a signal is sent to the magnetic door stop thereby releasing the door. In cases where there are multiple wildfire screens this becomes more and more practical as they could be readily interfaced with a fire control box and programmed to close all windows simultaneously.

1.5. Wildfire/Wild land infrared detector interfaced with a magnet door holding system.

1.5.1. **Conceptual Idea:** In this potential design an existing product (an infrared) detector would detect a bush fire. Traditionally the device will call the emergency services/fire department. We could conceptually interface this device with a device which would close the shutter (magnetic door holding system or a motor/reel.

Analysis: This is another type of detector that would be feasible when multiple windows were used. The factory listed lifespan of the detector is 20 years, which would make it possible to use with current cost constraints. Endurance tests for bush environment would need to be conducted to determine whether the lifespan was accurate or not. It is possible that if oriented correctly a single infrared detector would be able to protect the whole house. There is also the possibility of the detector being applicable for multiple fires, as long as it doesn't get damaged. False alarms are also a concern.

1.6. Pin Pull

1.6.1. **Conceptual Idea:** Heat responsive element is hooked up to a mechanism (spring that will release the line so the load of the line is not on the heat responsive element itself. See drawing.

Analysis: This design approaches the problem by taking the direct load of the door off the heat responsive element so it is possible that a cheaper or lower activation energy element could be used. The pin can be removed in a

variety of different methods, making it adaptable to different situations. Concerns are the possibility of the pin jamming if under a load, and the mechanism blocking radiation to the heat responsive element. Fusible links may also be the simpler option to a pin pull mechanism.

1.7.   Heat Expanding Metal (Bi-Metal detector)

1.7.1.   **Conceptual Idea:** Coil expands to push shutter closed. Eliminates the counter weight system (or minimizes the required size of the counter weight).

Analysis: This design could be used in two ways, to push the door closed, or to pull a pin. The more practical design would be the pin pull design as it would require a small amount of metal. The coil design would simplify the system making it less likely to fail. The concern with heat expanding metal is that on hot days the coil would partially close the fire shutter, and the pin design would partially pull out the pin, compromising the assembly.

1.8.   Nylon rope

1.8.1.   **Conceptual Idea:** Polypropylene ropes generally have melting temperatures in the range of 65 degrees C. This could be used as an alternative to fusible links, with the rope comprising of a small section of the wire or the entire length.

Analysis: This design would also be practical cheap alternative to the fusible link design. The concern with polypropylene rope would be the lifespan of the rope and ratio of diameter of rope needed to hold the load vs. ability to activate before critical heat flux.

1.9.   Ice cube

1.10.   **Conceptual Idea:** Have two wire ends with flat plates frozen into an ice block in a refrigeration unit that regularly refills with water to compensate for evaporation. Higher heat exposure and greater irradiation would melt the ice enough so it would break and the plates would come apart.

Analysis: This is an impractical idea that consists of an overcomplicated design that would take up a lot of energy. This design will not be considered for the possibility of being the final design but was part of the brainstorming session.

1.11. Compressed Gas in low hoop strength cylinder chamber

1.11.1.   **Conceptual Idea:** The radiant energy from the bush fire would heat a cylindrical container (containing a compressed gas) causing the gas to expand and eventually rupture the cylinder, freeing the assembly to move.

Analysis: This is a possible solution for the problem as well. The best design for this would be to have cylinder full of a liquid that has a phase change temperature in the range we are looking for. Gas would work as well but there is concern that with gas of false alarms, expanding of the canister, or puncture of the canister. This would also be a single use device, requiring the cylinder to be replaced after a fire.

1.12. Double paned window*(essentially 2 windows) interfaced with control

1.12.1.   **Conceptual Idea:** In this design there would essentially be two windows with a maintained pressure between them. When the first window breaks something would sense the pressure change thereby activating the fire

shutter. The windows would have two different types of glass with the more sensitive glass being exposed to the wildfire conditions.

    Analysis: This design may be more appealing to the homeowner with the design dually protecting the inner window against fire and raised energy efficiency inside of the house because of the double paned windows. The concern is that the window would have to be replaced after every fire. If the homeowner waited to replace the window and in the meantime propped open the shutter, the design is compromised allowing for fire entry if another occurs.

Brainstorm session:

Fusible Links-
- Use existing fusible links (Riley Air Control System's link (70 C) and Globe Technologies Corporation's link (57 C))
-Use fusible link to suspend counterweight so shutter will close faster when dropped (??)
-Attach fusible link to lever or pulley system to decrease load/ increase lifespan

If link cannot operate before critical flux, to lower activation energy/ temperature:
- Drill/punch/burn/ acid burn holes or divets/notches in link (decreasing surface area slows radiative HT, decreases mass increases conductive HT in link)
- Grind down sides of link
- Paint link a dark color in order to increase emissivity (pyrex paint)
- Grind down plates so they are thinner (thereby increasing the rate of heat transfer to the link)
- Ball peen surfaces to increase surface area (thereby increasing the rate of heat transfer to the link)
- Use a lower activation temp. solder (increases the operating time)
- Put a high conductive material cylinder around link as a heat collector
- Change orientation
- Increase load on link
- Change link geometry for max exposure (cylinder?)
- Put link in glass tube
- Situate link farther away from the house
- Volume/Area solder ratio (insert a non fusible alloy

Plastic/Polymer-
-Replace fusible link with a plastic ring
-use a plastic wedge/stopper to hold wheel of door open

Pin Pull-
- use a pin to connect anchored wire with wire connected to shutter. Pin can be manual release as well as have a mechanism attached that automatically pulls pin
- Pin itself could be the heat responsive element made of plastic or low melting point alloy, shackles highly conductive with low conductive wire attached
- Mechanism to pull pin could be spring loaded scissor configuration held open by a heat responsive element
- Use T-start heat detector to fire out pin.
- Use heat expanding metal attached to pin to pull pin out

Heat Detector-
-Use a linear heat detector attached to control panel to either surround perimeter of house or line windows. If used for the perimeter of the house wire could be moved to sit some distance away from the house. When triggered would break the circuit and either use magnets or some other type of device to break the wire.
 - Use a rate of rise heat detector hooked up to same system
-Use wild land/wildfire infrared detector hooked up to similar system as other heat detectors
- Heat expanding metal could be coiled and put in a heat collector tube and used to push shutter closed
-Heat expanding metal could be put under the far side of the bottom track raising the track during a fire and causing the shutter to roll closed.

Other Ideas-
-Polypropylene rope to hold shutter closed, has a low melting point
-have a cylinder filled with a compressed liquid with phase change at a certain temperature to gas connecting the wire to an anchor. So at the specified temperature the cylinder would explode into two pieces and release the shutter.
- Have each window be a double paned vacuum sealed window with the outside pane being float glass and the inside pane tempered glass. When failure of the outer window occurred the shutter would be triggered by electrical or mechanical means, preserving the inner window.

Appendix B: Response Time Index Derivation and Discussion

In order to better understand the concept of a plunge test and the RTI of a sprinkler the derivation of the RTI Equation (26) was evaluated. The basic equation for the response index is shown in Equation (26) (SFPE, 2002). Equation (27) was accounted for using the energy balance in this equation it is clear that determination of the RTI value is based solely on convective heating.

$$RTI = \tau \cdot \mu^{1/2}$$

μ = Gas Velocity (m/s)

$$\tau = \frac{m \cdot c_p}{h \cdot A}$$
(26)

m = mass (kg)

c_p = Specific Heat ($\text{J}/\text{kg} \cdot {}^\text{o}C$)

h = Convection Coefficient

A = Area

$$\frac{dT_E}{dt} = \frac{1}{\tau} \cdot (T_g - T_E)$$

T_E = Temperature of Link (${}^\text{o}C$) (27)

T_g = Temperature of gas (${}^\text{o}C$)

τ = Time constant

Equation (27) can be solved to yield the analytical solution shown in Equation (28). Based on this solution a value for the time constant τ can be determined. The RTI is normally determined experimentally using a plunge test (description to come later), in the plunge test the operating time of the sprinkler is recorded and used in Equation (29). This result can be used to calculate the RTI as shown in Equation (30).

$$T_E - T_o = (T_g - T_\infty) \cdot [1 - e^{-t/\tau}]$$

T_E = Temperature of Link (${}^\text{o}C$)

T_o = Initial Temperature of Link (${}^\text{o}C$)

T_g = Temperature of Gas (${}^\text{o}C$) (28)

T_∞ = Ambient Air Temperature (${}^\text{o}C$)

t = Time (seconds)

τ = Time Constant

$$\tau_o = \frac{t_r}{\ln\left[\dfrac{(T_g - T_\infty)}{(T_g - T_r)}\right]}$$

t_r = Experimental Response Time (sec)

T_g = Temperature of Gas in Plunge Test (^oC)

T_∞ = Temperature of Ambient Air (^oC)

T_r = Activation Temperature of Link (^oC)

(29)

$$RTI = \frac{t_r \cdot \mu_o^{1/2}}{\ln\left[\dfrac{(T_g - T_\infty)}{(T_g - T_r)}\right]}$$

t_r = Experimental Response Time (sec)

μ_o = Velocity of air in plunge test (m/s)

T_g = Temperature of Gas in Plunge Test (^oC)

T_∞ = Temperature of Ambient Air (^oC)

T_r = Activation Temperature of Link (^oC)

(30)

Appendix C: Test Data

6.1 Gas-Fired Radiant Panel Array Testing

Gas-Fired Radiant Panel Array Data

Test	Excel File	Radiation Profile	Side	Attachement Method	Link Manufacturer	Link Type	Initial Temperature (Link Temp and Ambient Temp)	Link Activation Temperature (Celsius)	Measured Surface Activation Temperature (Celsius)	View Factor	Emmisivity	V_{air} (m/s)	Applied Load (kg)	Activation Time (seconds)	
1	23_01_07 test1	Fast	Right	Plastic tie	Riley Air	-	30.1	70	60.65	1	0.4	7.9	10	74	Fa
			Left	Plastic tie	Riley Air	-	30.1	70	53.55	1	0.4	7.7	10	73	Fa
2	23_01_07 test2	Fast	Right	Insulated wire	Riley Air	-	30.7	70	75.75	1	0.4	6.55	10	75	Fa
			Left	Insulated wire	Riley Air	-	30.7	70	47.95	1	0.4	5.95	10	67	Fa
3	24_01_07-test1	Fast	Right	Metal shackle	Riley Air	-	28.4	70	84.8	1	0.4	6.3	10	95	
			Left	Metal shackle	Riley Air	-	28.4	70	64.45	1	0.4	6.4	10	90	
4	24_01_07-test2	Fast	Right	Plastic tie	Globe Technologies	A	28.6	57	102.95	1	0.4	7.62	10	92	Fa
			Left	Metal shackle	Globe Technologies	A	28.6	57	57.1	1	0.4	7.45	10	122	
5	24_01_07_test3	Fast	Right	Metal wire	Globe Technologies	A	30.1	57	84.1	1	0.4	7.7	10	100	

#	Test	Speed	Side	Material	Manufacturer	A/-								Notes
			Left	Metal shackle	Globe Technologies	A	30.1	57	61.15	1	0.4	6.5	10	114	
6	24_01_07_test4	Fast	Right	Metal wire	Globe Technologies	A	30.3	57	79.2	0.06	0.6	6.86	10	106	Links not ex
			Left	Metal wire	Riley Air	-	30.3	70	68.5	0.05	0.6	5.1	10	97	
7	25_01_07_test1	Fast	Right	Metal wire	Riley Air	-	25.6	70	59	1	0.92	8.46	10	71	
			Left	Metal wire	Riley Air	-	25.6	70	76.2	1	0.92	5.56	10	72	
8	25_01_07test2	Slow	Right	Metal wire	Riley Air	-	27.3	70	71.1	1	0.4	5.8	10	577	
			Left	Metal wire	Riley Air	-	27.3	70	75.75	1	0.4	5.6	10	571	
9	25_01_07test3	Slow	Right	Metal wire	Globe Technologies	A	28.6	57	74.3	1	0.4	7.2	10	607	
			Left	Metal wire	Globe Technologies	A	28.6	57	73.85	1	0.4	7.9	10	613	
10	25_01_07test4	Slow	Right	Metal wire	Riley Air	-	29.2	70	67.85	1	0.92	6.48	10	460	
			Left	Metal wire	Riley Air	-	29.2	70	63.45	1	0.92	5.84	10	475	
11	25_01_07test5	Slow	Right	Metal wire	Globe Technologies	A	30.1	57	76.55	0.06	0.6	6.64	10	558	Links not ex
			Left	Metal wire	Globe Technologies	A	30.1	57	80.6	0.06	0.6	7	10	575	Links not ex
12	31_01_07-T1	Slow	Right	Metal wire	Globe Technologies	A	28.8	57	62.5	1	0.92	7.53	10	382	

#	Test	Speed	Side	Material	Brand									
			Left	Metal wire	Globe Technologies	A	28.8	57	60.65	1	0.92	9.84	10	403
13	31_01_07-T2	Fast	Right	Metal wire	Globe Technologies	A	29.2	57	59.9	1	0.92	9.06	10	67
			Left	Metal wire	Globe Technologies	A	29.2	57	57.35	1	0.92	9.97	10	69
14	12_02_07test1	Fast	Right	Metal wire	Globe Technologies	K	30.7	57	64.2	1	0.92	7.7	10	63
			Left	Metal wire	Globe Technologies	K	30.7	57	60.9	1	0.92	5.16	10	67
15	12_02_07test2	Slow	Right	Metal wire	Globe Technologies	K	33.4	57	86.5	1	0.92	6.07	10	341
			Left	Metal wire	Globe Technologies	K	33.4	57	60.7	1	0.92	4.81	10	336
16	13_02_07test1	Slow	Right	Metal wire	Globe Technologies	K	31.2	57	77.35	1	0.92	7.73	10	397
			Left	Metal wire	Riley Air	-	31.2	70	62.9	1	0.92	9.15	10	392
17	21_02_07test1	Fast	Right	Metal wire	Riley Air	-	30.2	70	70.1	1	0.92	4.05	10	73
			Left	Metal wire	Riley Air	-	30.2	70	68.15	1	0.92	5.56	10	74
18	21_02_07test2	Fast	Right	Metal wire	Plastic zip tie	-	31.6	-	169.55	1	0.92	7.6	10	91
			Left	Metal wire	Plastic zip tie	-	31.6	-	61.2	1	0.92	3.91	10	68
19	21_02_07test3	Slow	Right	Metal wire	Riley Air	-	31.1	70	69.8	1	0.92		10	402

| | | | Left | Metal wire | Riley Air | - | 31.1 | 70 | 73.05 | 1 | 0.92 | | 10 | 413 | |

Heat of Fusion Testing

This table is the oven specifications and link activation times used in determining the change of phase parameter. Thes results of this testing are presented in the body of the report.

					Heat of Fusion Oven Test Data			
Test	Excel File	Link Manufacturer	Link Type	Link Activation Temperature (Celsius)	Average Oven Temperature (Celsius)	Applied load (kg)	Change of Phase Time (seconds)	Activation Time (seconds)
1	Riley-1	Riley Air	-	70	97.4	0.263	-	-
2	TypeA-1	Globe Technologies	A	57	82.3	0.263	70	85
3	TypeA-2	Globe Technologies	A	57	83.9	10	68	97
4	TypeK-1	Globe Technologies	K	57	74.790625	0.263	20	31
5	TypeK-2	Globe Technologies	K	57	64.22	10	117	159
6	TypeK-3	Globe Technologies	K	57	85.896923	10	53	64

Sample Calculation using Runge-Kutta

$$T_E = \frac{k1 + 2 \cdot k2 + 2 \cdot k3 + k4}{6} + T_o$$

$$k_1 = C_1\left[Radiation(t)\right](CHP) - C_2(T_{link}) + C_3 - C_4\left[T_{link}{}^4\right] + C_5 - C'(T_{link} - T_{ambient})$$

$$k_2 = C_1\left[Radiation(t)\right](CHP) - C_2(T_{link} + \frac{k_1}{2}) + C_3 - C_4\left[\left(T_{link} + \frac{k_1}{2}\right)^4\right] + C_5 - C'\left[\left(T_{link} + \frac{k_1}{2}\right) - T_{ambient}\right]$$

$$k_3 = C_1\left[Radiation(t)\right](CHP) - C_2(T_{link} + \frac{k_2}{2}) + C_3 - C_4\left[\left(T_{link} + \frac{k_2}{2}\right)^4\right] + C_5 - C'\left[\left(T_{link} + \frac{k_2}{2}\right) - T_{ambient}\right]$$

$$k_4 = C_1\left[Radiation(t)\right](CHP) - C_2(T_{link} + k_4) + C_3 - C_4\left[(T_{link} + k_4)^4\right] + C_5 - C'\left[(T_{link} + k_4) - T_{ambient}\right]$$

The C_1, C_2, C_3, C_4 and C_5 values are values which are constant in the equation, the values for these intermediate constants are represented in the following equations:

$$
\begin{cases}
C_1 = \dfrac{A_{face}}{\rho V c_p}(1000) \cdot \varepsilon \cdot mass \\[2ex]
C_2 = \dfrac{2hA_{face}}{\rho V c_p} \\[2ex]
C_3 = \dfrac{2hA_{face}}{\rho V c_p}(T_{ambient}) \\[2ex]
C_4 = \dfrac{A_{face} \cdot \varepsilon \cdot \sigma}{\rho V c_p} \\[2ex]
C_5 = \dfrac{A_{face} \cdot \varepsilon \cdot \sigma}{\rho V c_p}(T_{ambient})
\end{cases}
$$

In this sample calculation used to verify the excel model a Globe Technologies Model A Link will be considered. Required user inputs into the model include the following:

Input Parameters Globe Technologies Link (57°C)		
Input	**Value**	**Units**
Air temperature=	30	C
Wind Speed=	9.06	m/s
Length=	0.03054	m
Width=	0.02155	m
Thickness=	0.003	m
Emissivity=	0.92	Unit-Less
Mass=	0.0121	kg
Viscosity=	0.00001589	Unit-Less
Pr=	0.709	Unit-Less
k_{air}=	0.0263	W/mK
c_p=	385	J/kgK
s-b const	5.67E-08	W / m K^4

- Incident Radiation: Fast Profile $\rightarrow$ $2.3105e^t$

Inserting the equation governing the incident radiation the equations for k1, k2, k3 and k4 are changed to be the following:

$$
k_1 = C_1\left[2.3105e^t\right](CHP) - C_2(T_{link}) + C_3 - C_4\left[T_{link}{}^4\right] + C_5 - C'(T_{link} - T_{ambient})
$$

$$
k_2 = C_1\left[2.3105e^{(t+0.5\cdot\Delta t)}\right](CHP) - C_2(T_{link} + \frac{k_1}{2}) + C_3 - C_4\left[\left(T_{link} + \frac{k_1}{2}\right)^4\right] + C_5 - C'\left[\left(T_{link} + \frac{k_1}{2}\right) - T_{ambient}\right]
$$

$$
k_3 = C_1\left[2.3105e^{(t+0.5\cdot\Delta t)}\right](CHP) - C_2(T_{link} + \frac{k_2}{2}) + C_3 - C_4\left[\left(T_{link} + \frac{k_2}{2}\right)^4\right] + C_5 - C'\left[\left(T_{link} + \frac{k_2}{2}\right) - T_{ambient}\right]
$$

$$
k_4 = C_1\left[2.3105e^{(t+\Delta t)}\right](CHP) - C_2(T_{link} + k_4) + C_3 - C_4\left[(T_{link} + k_4)^4\right] + C_5 - C'\left[(T_{link} + k_4) - T_{ambient}\right]
$$

Prior to calculating the values of k1, k2, k3 and k4 intermediate values of A_{face}, Volume, Density (ρ), Volume, the Reynold's Number, the Nusselt Number, the convective heat transfer coefficient (h) must be determined. Additionally values for the conductance (C') and heat of fusion energy (CHP) must be determined experimentally or approximated and

98

input into the thermal response model. For these values a C' value of 0.003553 will be used and a CHP value of 0.8615 will be used.

$$A_{face} = Length \times Width$$
$$A_{face} = (0.0305m \times 0.02155m)$$
$$A_{face} = 0.000658m^2$$

$$V = Length \times Width \times Thickness$$
$$V = 0.0305m \times 0.02155m \times 0.003m)$$
$$V = 1.97 \times 10^{-6} m^3$$

$$Density = \frac{mass}{V} = \frac{0.121kg}{1.97 \times 10^{-6} m^3}$$
$$Density = 6128.4 \frac{kg}{m^3}$$

$$Characteri sticLength = \frac{Volume}{A_{face}}$$
$$Characteri sticLength = \frac{1.97 \times 10^{-6} m^3}{0.000658 m^3}$$
$$Characteri sticLength = 0.003m$$

$$Re_D = \frac{\mu \cdot D}{v}$$
$$Re_D = \frac{\left(9.06 \frac{m}{s}\right)(0.003m)}{0.00001589\left(\frac{m^2}{s}\right)}$$
$$Re_d = 1710.509$$

$$\overline{Nu}_D = C \cdot Re_D^m \cdot Pr^{1/3}$$
$$\overline{Nu}_D = 0.228 \cdot 1710.509^{0.731} \cdot 0.709^{\left(1/3\right)}$$
$$\overline{Nu}_D = 12.24$$

$$\bar{h} = \overline{Nu}_D \cdot \left(\frac{k}{D}\right)$$

$$\bar{h} = 12.24 \cdot \left(\frac{0.0263 \, W/m \cdot {}^oC}{0.003 m}\right)$$

$$\bar{h} = 107.338552 \left(W/m^2 \cdot {}^oC\right)$$

$$C_1 = \frac{A_{face}}{\rho V c_p}(1000) \cdot \varepsilon \cdot mass$$

$$C_1 = \frac{\left(0.000658 m^2\right)}{\left(6128.4 \, kg/m^3\right)\left(1.97 \times 10^{-6} m^2\right)\left(385 \, J/kg \cdot {}^oC\right)}(1000) \cdot 0.9 \cdot (0.0121 kg)$$

$$C_1 = 0.1095388$$

$$C_2 = \frac{2hA_{face}}{\rho V c_p}$$

$$C_2 = \frac{2\left(107.338552 \, W/m^2 \cdot {}^oC\right)\left(0.000658 m^2\right)}{\left(6128.4 \, kg/m^3\right)\left(1.97 \times 10^{-6} m^3\right)\left(385 \, J/kg \cdot {}^oC\right)}$$

$$C_2 = 0.03032885$$

$$C_3 = \frac{2hA_{face}}{\rho V c_p}\left(T_{ambient}\right)$$

$$C_3 = \frac{2\left(107.338552 \, W/m^2 \cdot {}^oC\right)\left(0.000658 m^2\right)}{\left(6128.4 \, kg/m^3\right)\left(1.97 \times 10^{-6} m^3\right)\left(385 \, J/kg \cdot {}^oC\right)}\left(31.5{}^oC\right)$$

$$C_3 = 0.955358$$

$$C_4 = \frac{A_{face} \cdot \varepsilon \cdot \sigma}{\rho V c_p}$$

$$C_4 = \frac{\left(0.000658 m^2\right) \cdot (0.9) \cdot \left(5.67 \times 10^{-8} \, W/m^4 \cdot {}^oC\right)}{\left(6128.4 \, kg/m^3\right)\left(1.97 \times 10^{-6} m^3\right)\left(385 \, J/kg \cdot {}^oC\right)}$$

$$C_4 = 7.20934 \times 10^{-12}$$

$$C_5 = \frac{A_{face} \cdot \varepsilon \cdot \sigma}{\rho V c_p} (T_{ambient})$$

$$C_5 = \frac{\left(0.000658 m^2\right) \cdot (0.9) \cdot \left(5.67 \times 10^{-8} W/m^{4 \cdot o}C\right)}{\left(6128.4 \, kg/m^3\right)\left(1.97 \times 10^{-6} m^3\right)\left(385 \, J/kg \cdot {}^oC\right)} \left(31.5^o C\right)$$

$$C_5 = 7.09803 \times 10^{-6}$$

After calculating these intermediate values and determining the CHP and C' parameters experimentally, these results are plugged into the k1, k2, k3, and k4 equations to solve the problem.

$$k_1 = C_1 \left[2.3105 \, e^t\right](CHP) - C_2 (T_{link}) + C_3 - C_4 \left[T_{link}^{\,4}\right] + C_5 - C'(T_{link} - T_{ambient})$$

$$k_1 = (0.1095388)\left[2.3105 \, e^0\right](0.8615) - (0.03032885)(31.5) + (0.955358)$$
$$- \left(7.20934 \times 10^{-12}\right)\left[\left(31.5^o C\right)^4\right] + \left(7.09803 \times 10^{-6}\right) - (0.003553)(31.5^o C - 31.5^o C)$$

$$k_1 = 0.25308$$

$$k_2 = C_1\left[2.3105 e^{(t+0.5 \cdot \Delta t)}\right](CHP) - C_2 \left(T_{link} + \frac{k_1}{2}\right) + C_3 - C_4 \left[\left(T_{link} + \frac{k_1}{2}\right)^4\right] + C_5 - C'\left[\left(T_{link} + \frac{k_1}{2}\right) - T_{ambient}\right]$$

$$k_2 = (0.1095388)\left[2.3105 e^{0+0.5}\right](0.8615) - (0.03032885)(31.5^o C + \frac{0.25308}{2}) + (0.955358)$$
$$- \left(7.20934 \times 10^{-12}\right)\left[\left(31.5^o C + \frac{0.25038}{2}\right)^4\right] + \left(7.09803 \times 10^{-6}\right) - (0.003553)\left(31.5^o C + \frac{0.25038}{2}\right) - 31.5^o C)$$

$$k_2 = 0.252569$$

$$k_3 = C_1\left[2.3105 e^{(t+0.5 \cdot \Delta t)}\right](CHP) - C_2 \left(T_{link} + \frac{k_2}{2}\right) + C_3 - C_4 \left[\left(T_{link} + \frac{k_2}{2}\right)^4\right] + C_5 - C'\left[\left(T_{link} + \frac{k_2}{2}\right) - T_{ambient}\right]$$

$$k_3 = (0.1095388)\left[2.3105 e^{0+.5}\right](0.8615) - (0.03032885)(31.5^o C + \frac{0.252569}{2}) + (0.955358)$$
$$- \left(7.20934 \times 10^{-12}\right)\left[\left(31.5^o C + \frac{0.252569}{2}\right)^4\right] + \left(7.09803 \times 10^{-6}\right) - (0.003553)\left(31.5^o C + \frac{0.252569}{2}\right) - 31.5^o C)$$

$$k_3 = 0.252769$$

$$k_4 = C_1 \left[2.3105 e^{(t+\Delta t)} \right] (CHP) - C_2 (T_{link} + k_4) + C_3 - C_4 \left[(T_{link} + k_4)^4 \right] + C_5 - C' \left[(T_{link} + k_4) - T_{ambient} \right]$$

$$k_4 = (0.1095388) \left[2.3105 e^{0+1} \right] (0.8615) - (0.03032885)(31.5^o C + 0.252769) + (0.955358)$$
$$- \left(7.20934 \times 10^{-12} \right) \left[(31.5^o C + 0.252769)^4 \right] + \left(7.09803 \times 10^{-6} \right) - (0.003553) \left((31.5^o C + 0.252769) - 31.5^o C \right)$$

$$k_4 = 0.252478$$

Now with the determined values of k1, k2, k3 and k4 it is possible to determine the temperature of the link at 1 second, this calculation is shown below:

$$T_E = \frac{k1 + 2 \cdot k2 + 2 \cdot k3 + k4}{6} + T_o$$

$$T_E = \frac{(0.25308) + 2(0.252569) + 2(0.252769) + (0.2524)}{6} + 31.5^o C$$

$$T_E = 31.7527^o C$$

This calculation matches the result of the calculated results of the thermal response model. The calculation procedures are then repeated with the time (t) equal to 1 second and the temperature T_{link} equal to the previously determined temperature. This is the numerical method used to account for the transient nature of the problem.